Pathological study on canine immune-mediated meningoencephalomyelitis

イヌの免疫介在性髄膜脳炎に関する病理学的研究

Eunsil Park

朴　琅　實

Contents

General Introduction----------3

Chapter I ----------7

Comprehensive immunohistochemical studies on canine necrotizing meningoencephalitis (NME), necrotizing leukoencephalitis (NLE), and granulomatous meningoencephalomyelitis (GME).

Chapter II----------30

Th1-, Th2- and Th17-related cytokine and chemokine receptor mRNA and protein expression in brain tissues, T cells and macrophages in dogs with necrotizing and granulomatous meningoencephalitis

Chapter III----------49

Establishment of rodent model for canine necrotizing meningoencephalitis (NME), necrotizing leukoencephalitis (NLE), and granulomatous meningoencephalomyelitis (GME).

Conclusions----------77

Acknowledgement----------81

Reference----------82

General Introduction

Canine idiopathic encephalitis includes two distinct disorders, necrotizing encephalitis (NE) and granulomatous meningoencephalomyelitis (GME). NE is characterized by prominent necrosis and the infiltration of inflammatory cells including lymphocytes, plasma cells and macrophages. NE is divided into two subtypes, necrotizing meningoencephalitis (NME) and necrotizing leukoencephalitis (NLE) according to the distribution of the lesions. In most of NME cases, necrosis and inflammatory cell infiltration are located in the hippocampus, thalamus and leptomeninges as well as in the cerebral cortex and subcortical region. NME has been reported in various canine breeds including the pug [11, 19, 47, 55], Maltese [26, 68, 85], Shih-tzu [90], papillon [88], Chihuahua [36] and Pekingese [18]. Meanwhile, in a few breeds, such as the Yorkshire terrier [5, 24, 50, 57, 91, 93] and French bulldog [84], the lesions are predominately observed in the cerebral white matter, and the disease is called necrotizing leukoencephalitis (NLE). Accordingly, NME and NLE seem to be breed-specific, respectively. The age of the onsets of NME and NLE varies, but tends to be as early as 9 years, with some exceptions. Most of the affected dogs show generalized seizures, head tilt, circling, depression and sometimes visual defects.

GME is the other idiopathic canine CNS disorder that is characterized by granulomatous lesions containing epithelioid cells, and perivascular cuffs composed of lymphocytes, plasma cells, macrophages and some neutrophils mainly in the cerebellum and brain stem [1, 27, 28, 43, 44, 45, 88, 89, 90]. GME has been considered to be an inflammatory form of reticulosis, which is characterized by the proliferation of reticulohistiocytes derived from the leptomeninges or microglial cells [89]. Reticulosis was categorized into three types; 1) inflammatory reticulosis, 2) neoplastic reticulosis and 3) microgliomatosis. Inflammatory reticulosis was composed of

reticulohistiocytes, lymphocytes, plasma cells and other leukocytes, whereas neoplastic reticulosis was of monomorphic neoplastic cells. At the present, although it is still controversial, GME is considered a variant inflammatory reticulosis. Furthermore, there are three types of GME according to the localization of lesions; 1) ocular form, 2) focal form and 3) disseminated form [85]. GME has been reported in dogs of various breeds and ages. Female dogs are more susceptible than male dogs [87]. Clinical signs are various reflecting the site of lesions, such as facial paralysis, circling, head tilt, depression, nystagmus, blindness with abnormal papillary light reflexes and cervical pain.

Given the etiology and the pathophysiology, NE and GME seem to be different diseases. However, I have observed a few GME cases that did not display prominent granulomatous lesions, and a few rare cases involved in the cerebral cortex and white matter. Also, the characteristic malacic changes were not observed in some acute NME or NLE cases, only with leptomeningitis. Differential diagnoses for NME should therefore be considered.

The etiopathogeneses of NME, NLE and GME still remain unclear, although many previous reports have tried to identify their causes [5, 30, 59, 66, 69, 76, 81, 88, 89, 92]. Because of the failure of the detection of pathogens in NME, NLE or GME cases in previous reports, the direct relation to certain specific pathogens could be hardly supported. Some reports have suggested that these conditions are autoantibody-mediated [81, 90, 92] or T cell-mediated [43, 88, 89]. Although autoantibodies against glial fibrillary acid protein (GFAP) have been detected in the cerebrospinal fluid (CSF) of many dogs with NME, they may not be specific to NME and were absent in some cases [59, 81]. It is therefore disputed whether autoantibodies against GFAP are a cause or secondary products of NME. Suzuki *et al*. reported that CD3-positive T cells

predominate in NME and GME lesions [88, 89] and suggested that GME is a form of delayed type hypersensitivity based on an autoimmune response [43]. Thus, the T cell response may play a key role in NME, NLE and GME.

The definitive diagnosis of NME, NLE and GME has been based on the characteristic histopathological lesions. In recent, tentative diagnoses of the diseases are possible by computed tomography (CT) or magnetic resonance imaging (MRI) system. Additionally, the detection of anti-GFAP autoantibodies in the CSF is useful for the possible diagnosis readily. Since these diseases have been considered immune-mediated disorders, these have been treated and maintained with immunosuppressive drugs. By such reasons, studies on the cause and pathogenesis of these diseases have decreased, while studies on the genetic background have been paid attention in recent. Thus, there are needs to investigate whether NME, NLE and GME are different diseases, and what the nature of inflammatory reactions of these diseases is. In addition, it should be confirmed whether these diseases are autoimmune-mediated and produced by self-antigens, using experimental models.

This thesis is composed of 3 chapters. In the Chapter 1, the distinct lesions and their localizations in NME, NLE and GME cases were compared, and the infiltrated inflammatory cells among three diseases were identified and quantified. In NME and NLE cases, the relations with astrocytes and the T cells or IgG were demonstrated. In the Chapter 2, the mRNA and protein levels of the distinct cytokines and chemokine receptors in the three diseases were examined with fresh frozen brain tissues. The inflammatory cells that produced and/or secreted the cytokines were identified and quantified. In the Chapters 1 and 2, the similarities and the differences of inflammatory reactions among the diseases were confirmed, and the relation to distinct lesions was also discussed. In the Chapter 3, experimental animal models for NME,

NLE and GME were sought with LEW rats injected with a rat cerebrum homogenate or the rat cerebellum homogenate, and the pathogenesis was discussed.

Chapter I

Comprehensive immunohistochemical studies on canine necrotizing meningoencephalitis (NME), necrotizing leukoencephalitis (NLE) and granulomatous meningoencephalomyelitis (GME)

Summary

In dogs, there are several idiopathic meningoencephalitides, such as necrotizing meningoencephalitis (NME), necrotizing leukoencephalitis (NLE), and granulomatous meningoencephalomyelitis (GME). Although they are often assumed to be immune-mediated, the etiology of these diseases remains elusive. In this study, the histopathology of the lesions caused by these conditions and the inflammatory cell populations produced in response to them were examined among dogs affected with GME, NME, or NLE in order to understand their pathogeneses. The brain tissues of dogs with NME (n=25), NLE (n=5), or GME (n=9) were used. The inflammatory cells were identified by immunohistochemistry using antibodies against CD3, IgG, CD20, CD79acy, and CD163. In NME and NLE, malacic changes were located in the cerebral cortex, and the cerebral white matter and thalamus, respectively. The distribution of the brain lesions in NME and NLE was breed-specific. In GME, granulomatous lesions that were mostly composed of epithelioid macrophages were observed in the cerebral white matter, cerebellum, and brain stem. Although the proportions of IgG-, CD20-, and CD79acy-positive cells (B cells) were not significantly different among the GME, NME, and NLE lesions, that of CD3-positive cells (T cells) was increased in GME. In NME and NLE, CD163-positive cells (macrophages) had diffusely infiltrated the cerebral cortex and white matter, respectively. However, in GME, CD163-positive cells accumulated around the blood vessels in the cerebral and cerebellar white matter. The distributions of these pathologic lesions were quite different among GME, NME, and NLE, whereas there were no marked differences in the proportions of inflammatory cells.

Introduction

Necrotizing non-suppurative meningoencephalitis (NME) is an idiopathic inflammatory disease of the canine central nervous system (CNS) that is characterized by prominent necrosis and the infiltration of inflammatory cells including lymphocytes, plasma cells, and monocytes or histiocytes into the cerebral cortex and/or white matter, hippocampus, thalamus, and leptomeninges. NME has been reported in various canine breeds including the pug [11, 19, 47, 55], Maltese [25, 68, 85], Shih-tzu [88], papillon [88], Chihuahua [36], Pekingese [18], Yorkshire terrier [5, 24, 50, 57, 91, 93], and French bulldog [84]. The areas of necrosis and inflammatory cell infiltration are localized in the cerebral cortex and subcortical region in most NME cases, whereas, in a few breeds, such as the Yorkshire terrier and French bulldog, the lesions are predominately observed in the white matter, and the disease is called necrotizing leukoencephalitis (NLE).

Granulomatous meningoencephalomyelitis (GME) is another idiopathic canine CNS disorder that is characterized by perivascular cuffs composed of lymphocytes, plasma cells, macrophages, and some neutrophils, and granulomatous lesions containing epithelioid cells, mainly in the cerebellum and brain stem [1, 27, 28, 43, 44, 45, 88, 89, 90]. However, we have observed a few GME cases that did not display prominent granulomatous lesions, perivascular cuffs, or inflammatory cell infiltration, and rare cases involved the cerebral cortex and white matter. Differential diagnoses for NME should therefore be considered.

The etiopathogeneses of NME, NLE, and GME remain unclear, although many previous reports have tried to identify their causes [5, 30, 59, 66, 69, 76, 81, 88, 89, 92]. In a few cases of GME, the involvement of Borna virus [66, 94] or West Nile virus [90] was suspected. In NME and NLE cases, the influence of RNA viruses, such as canine

distemper virus, herpes virus, and rabies virus, has also been examined [11, 16, 18, 36, 47, 57, 76, 84, 88, 91]. However, no viruses were detected by PCR in paraffin-embedded brain tissues from dogs with NME, NLE, or GME [76]. Some reports have suggested that these conditions are autoantibody-mediated [81, 90, 92] or T cell-mediated [43, 88, 89]. Although autoantibodies against glial fibrillary acid protein (GFAP) have been detected in the cerebrospinal fluid (CSF) of many dogs with NME, they were not specific to NME and were absent in some cases [59, 81]. It is therefore disputed whether autoantibodies against GFAP are a cause or secondary products of NME. Suzuki et al. reported that CD3-positive T cells predominate in NME and GME lesions [88, 89] and suggested that GME is a form of delayed type hypersensitivity based on an autoimmune response [43]. Thus, the T cell response may play a key role in NME, NLE, and GME.

NME, NLE, and GME are considered to be different diseases because of their unique characteristic lesions, localization in the brain, and breed specificities. Therefore, to confirm whether they are different, the dominant inflammatory cell populations of the diseases should be compared. Thus, in the present study, we compared the lesions, lesion locations, and inflammatory cell populations of NME, NLE, and GME.

Materials and Methods

Dog brains

The brain tissues of dogs with NME, NLE, and/or GME were obtained during necropsies performed between 1990 and 2009 at our laboratory. The brains from 25 NME, 5 NLE, and 9 GME cases were examined (Table 1).

Pathological examinations

Brain tissues were fixed in 10% neutral buffered formalin, and selected tissues were subsequently routinely embedded in paraffin, sectioned at 4㎛, and stained with hematoxylin and eosin (HE), HE-Luxol fast blue (HE-LFB), and toluidine blue (TB) for microscopic examinations. Other fresh brain tissues from 2 dogs with NME and 1 dog with GME were frozen in Tissue-Tek O.C.T. Compound (Sakura Finetek Japan, Tokyo, Japan) and subsequently stored at -80°C.

Immunohistochemistry

For antigen retrieval, deparaffinized sections were autoclaved at 121°C for 15 min or digested with proteinase K (1:400, Wako, Osaka, Japan) at 37°C for 30 min. Additionally, for the CD79acy immunostaining, sections were treated with 1% sodium dodecyl sulfate (SDS) at room temperature for 5 min and then treated with hyaluronidase (4,000 U/ml, Sigma, St. Louis, MO, U.S.A.) at 37°C for 30 min. Endogenous peroxidase activity was blocked by incubating the sections with 3% hydrogen peroxide in methanol at room temperature for 5 min. For the tissue blocking, the sections were further treated with skimmed milk at 37°C for 40 min. The sections were then incubated at 37°C for 1 hr or at 4°C overnight with primary antibodies. The primary antibodies employed are listed in Table 2. Thereafter, the sections were incubated with the Envision polymer reagent (DAKO Japan, Kyoto, Japan) or the LSAB reagent (DAKO Japan) at room temperature for 40 min. Visualization was performed with 3,3’-diaminobenzidine tetrahydrochloride (Wako), and counterstaining was performed with hematoxylin.

Quantitative data analysis

The numbers of CD3-, IgG-, CD20-, CD79acy-, and CD163-positive cells per 200 mononuclear cells were counted under x 400 magnification in 10 selected fields of perivascular cuff lesions and areas displaying parenchymal infiltration. Then, mean cell percentage and standard deviation values were calculated. Mean values were compared using the Student's *t*-test.

Double-labeling immunofluorescence

Six μm thick-paraffin sections were autoclaved at 121°C for 15 min for antigen retrieval and treated with skimmed milk at 37°C for 40 min to block nonspecific reactions. The first primary antibodies were employed at 4°C overnight. The first primary antibodies were rabbit polyclonal antibodies against human CD3 (Dako, Japan) and biotinylated sheep antiserum against canine IgG (American Qualex, San Clemente, CA, U.S.A.). The sections were then incubated with the second primary antibody, mouse monoclonal against human glial filament protein (GFP, prediluted, PROGEN, Heidelberg, Germany), at 37°C for 1 hour. The secondary antibody cocktail was employed at room temperature for 1 hour. The cocktail included fluorescein isothiocyanate–labeled goat anti-rabbit IgG (1:200, Vector Laboratories, Burlingame, CA, U.S.A.), fluorescein streptavidin (1:200, Vector Laboratories), and Alexa fluor 594-labeled goat anti-mouse IgG (1:200, Invitrogen, Eugene, OR). Fluorescein streptavidin was used to visualize the first biotinylated canine IgG antibody. The sections were finally counterstained with TO-PRO-3 iodide (1:1000, Invitrogen, Camarillo, CA) at room temperature for 30 min, mounted with Vectashield HardSet (Vector Laboratories), and observed using the Zeiss LSM 510 confocal laser scanning microscope.

Results

Breed specificities

Different from GME, NME and NLE tended to be breed-specific and usually occurred in small breeds. Pug, Chihuahua, Maltese, and papillon dogs were often affected by NME (Table 1, Fig. 1A). Yorkshire terriers and some pugs were more likely to be affected by NLE (Table 1, Fig. 1C). One papillon with NME developed malacic lesions in both the cerebral cortex and white matter.

Pathological changes

[NME]

Among the microscopic findings of NME, malacic changes and inflammatory lesions were most prominent in the cerebral cortex, hippocampus, and thalamus (Table 3, Table 4, Fig. 1B). In addition, endothelial hyperplasia or microgliosis were also observed in the capsula interna, nucleus geniculatus medialis, nucleus caudatus, crus cerebri, pons, nuclei habenulares, nucleus pretectalis, and the cerebral cortex in several cases.

The histopathological lesions of the NME dogs examined were divided into three phases: acute, subacute, and chronic. The acute phase lesions were mainly composed of regions of mild inflammatory cell infiltration. Moderate malacic changes and intense inflammatory reactions were observed in the subacute phase (Figs. 2A, 2B). In the chronic phase, extensive malacic changes predominated. Areas of leptomeningeal infiltration and perivascular cuffs were most commonly observed in the subacute phase, while they were also found in the chronic phase accompanied with extensive necrosis. The inflammatory reactions progressed continuously throughout the progression of the disease.

[NLE]

Lesions were found in the thalamus of the majority of NLE cases and in the hippocampus, mesencephalon, cerebellum, and spinal cord in a few cases (Table 3, Table 4). The capsula interna was affected in one case.

Malacic changes were specifically found in the cerebral white matter and subcortical region (Fig. 1C), and inflammatory lesions (Figs. 1D, 2C, 2D) were located in similar regions to those in which they were found in NME. Different from NME, the subleptomeningeal lesions and astrogliosis were mild to moderate. Inflammatory cell infiltration was prominent in the ependyma and mild in the choroid plexus. Vacuolar changes, swollen or fragmented myelin fibers, and spheroid formation were found in the peripheral malacic regions.

[GME]

Characteristically angiocentric or nodular granulomatous lesions (Figs. 1F, 2E, 2F) composed of macrophages, epithelioid cells, lymphocytes, plasma cells, and neutrophils were observed in the cerebellum, medulla oblongata, and spinal cord (Table 3, Table 4). Lesions were detected in the cerebral white matter, especially in subcortical regions, such as the mesencephalon and thalamus (Fig. 1E).

Perivascular cuff lesions as well as those involving leptomeningeal infiltration, astrogliosis, and microgliosis were multifocal and asymmetric. The perivascular cuffs consisted of lymphocytes, plasma cells, macrophages, neutrophils, and hypertrophic endothelial cells. Areas of leptomeningeal infiltration were prominent in the cerebellum, brain stem, and spinal cord, especially in the sulci, but mild in the cerebrum. Astrogliosis and microgliosis were frequently detected in the active and severe inflammatory lesions. Malacic lesions were observed in a few cases, which were milder than those found in NME.

Quantification of inflammatory cells

Immunohistochemistry was used to quantify the number of inflammatory cells as illustrated in Figs. 13-22. CD3-positive T cells in the perivascular cuffs, neuroparenchymal, and leptomeningeal lesions were predominant among the inflammatory cell populations in the order of GME, NLE, and NME, and the proportions of these cells were significantly different between the diseases (Figs. 3A, 3D, 3G, 4). However, there were few CD3-positive T cells in the malacic regions of NME and NLE.

In this study, IgG, CD20, and CD79acy were used as B cell markers. CD20 is present in the cell membrane of late pro-B cells through memory cells, but not plasma cells, while IgG is present in the cytoplasm of plasma cells. CD79acy is expressed in the cell membrane throughout B cell life cycle, as well as active plasma cells. The proportion of IgG-positive plasma cells and CD20- and CD79acy positive B cells was not significantly different (Figs. 3B, 3E, 3H, 4). CD20-positive B cells were more frequently observed in the perivascular cuffs than in the neuroparenchyma, while IgG-positive plasma cells and CD79acy-positive B cells infiltrated similarly in the perivascular cuffs and in the neuroparenchyma (Figs. 3B, 3E, 3H, 4).

We then used CD163 as a macrophage and epithelioid cell marker as it is slightly more specific than other anti-macrophage antibodies such as anti-myeloid/histiocyte antigen (MAC387), lysozyme, Iba-1, and macrophage (HAM56). CD163-positive macrophages were observed more frequently in the GME lesions, particularly in the perivascular cuffs, than in those observed in NME and NLE (Figs. 3C, 3F, 3I, 4). In NME, NLE, and GME, CD163-positive macrophages were localized in the active inflammatory lesions such as the perivascular cuffs and areas of neuroparenchymal infiltration (Figs. 3C, 3F, 3I). In NME and NLE, they were mainly

found in the cerebral cortex and white matter, particularly in necrotic lesions, and rarely in the cerebellum, brain stem, and spinal cord. On the other hand, in GME, they were mostly observed in the cerebellum, brain stem, spinal cord, and cerebral white matter. CD163-positive epithelioid cells were specifically detected in the granulomatous lesions of GME, but not NME or NLE (Fig. 3I).

The proportion of myeloperoxidase-positive neutrophils was approximately 5~10%, although no suppurative lesions were found in NME, NLE, or GME (data not shown). Neutrophils were mainly located in the necrotic, perivascular cuff, neuroparenchymal, and leptomeningeal lesions, and they were also frequently observed in the granulomatous GME lesions.

Double-labeling immunofluorescence

[CD3 and GFAP]

In the NME lesions, many CD3-positive T cells (green) adhered to GFAP-positive astrocytes (red) in the peripheral malacic regions of the cortex (Fig. 5A). However, in the NLE and GME lesions, CD3-positive T cells had infiltrated among the fibrous processes of GFAP-positive astrocytes in the white matter (Fig. 5C).

[IgG and GFAP]

The cytoplasm and/or processes of some astrocytes were labeled with both IgG and GFAP (yellow) in both NME (Fig. 5B) and NLE (Fig. 5D), but not in GME. These double-positive astrocytes were more prominent in NME than NLE and were frequently observed in the leptomeninges and the periphery of the lesions displaying necrosis and astrogliosis.

Discussion

In the present study, the brain lesions observed in pug, papillon, Chihuahua, and Maltese dogs with NME were mainly characterized by cerebral cortical lesions such as malacia, perivascular cuffs, and the neuroparenchymal infiltration of inflammatory cells. The lesions were located in the white matter as well as the cerebral cortex in a few pug, papillon, and Chihuahua dogs. In contrast, similar brain lesions were localized in the white matter of Yorkshire terriers with NLE. Thus, the distribution of NME and NLE lesions seems to be breed-specific. On the contrary, in dogs with GME the characteristic granulomatous lesions were mostly located in the cerebellum, brain stem, and spinal cord, and additional non-granulomatous inflammatory lesions were found in the cerebral white matter and mesencephalon. Consequently, in NME and NLE the histopathological lesions are malacic or inflammatory and are found in the prosencephalon and parts of the mesencephalon, whereas those found in GME are granulomatous or inflammatory and are usually located in the rhombencephalon. The distribution of the lesions in these canine brain inflammatory diseases was consistent with that described in previous reports [1, 5, 11, 18, 19, 23, 24, 26, 27, 28, 36, 43, 44, 45, 47, 50, 55, 57, 68, 69, 84, 85, 88, 89, 90, 91, 93].

In a comparison of the inflammatory cell populations among NME, NLE, and GME, CD3-positive T cells were found to be the most prominent inflammatory cells in these diseases and were most often observed in the GME lesions, followed by those of NLE and NME, confirming the results of previous reports [28, 36, 43, 45, 84, 88, 89, 90]. CD163-positive macrophages were more predominant in GME than in NME or NLE, although the difference was not significant. It is plausible that the macrophages that infiltrate into the malacic lesions in the brains of dogs with NME or NLE act as scavenger cells that remove malacic or inflammatory products [58]. In contrast, the

macrophages in GME lesions are thought to form granulomatous lesions as part of an immune response [43, 55, 58, 88, 90]. In this study, the proportion of IgG-positive plasma cells and CD20- and/or CD79acy-positive B cells was not significantly different among NME, NLE, and GME. B cells seemed to infiltrate into the neuroparenchyma less than plasma cells since CD20-positive B cells were observed more in the perivascular cuffs than in the neuroparenchyma. The proportion of inflammatory cells did not differ significantly among NME, NLE, and GME, although there were marked differences in the histopathology of the lesions and their locations. Taken together, these results suggest that these diseases share a common pathogenesis in dogs.

This retrospective study has several limitations such as variability in disease duration and treatment. The majority of cases had been diagnosed presumptively as NME, NLE or GME through clinical signs, autoantibody test, computed tomography (CT) or magnetic resonance imaging (MRI). The dogs were treated with immunosuppressive drugs, such as corticosteroids (prednisone, prednisolone, and dexamethasone) and anticonvulsants such as phenobarbital and pentobarbital. They died or were euthanized due to poor response to the treatment, and a definitive diagnosis was made with NME, NLE, and GME through the histopathological examination. Corticosteroids such as dexamethasone and prednisone inhibit T cell- or macrophage-mediated immunity, production of cytokines, and partial B cell-mediated immunity [14, 21, 22, 41, 56, 67, 86]. This study was performed with the cases which progressed acutely or chronically despite continuous treatment and maintenance. Certainly, some degree of inflammatory reactions could have been affected by corticosteroids. However, inflammatory reactions of cases in this study were active, and characteristic lesions such as malacic or granulomatous changes were observed. This suggests that the nature of the inflammatory reactions was not significantly distorted by treatment.

Double-labeling IFA was performed to identify the targets of inflammatory cells. CD3-positive T cells were found in close proximity or attached to astrocytes, and the cytoplasm and astrocytic processes were positive for IgG in NME and NLE lesions, although the distribution of the lesions differed among the diseases. These IgG-positive astrocytes were more prominent in NME than in NLE. Since NME prominently affects the cerebral gray matter, which is composed of protoplasmic astrocytes, and NLE affects the white matter, which is composed of fibrous astrocytes, the difference in the lesion distribution between NME and NLE can be attributed to the targets of autoantibodies against protoplasmic astrocytes or fibrous astrocytes [60, 97]. In addition, since astrogliosis was more significant in NME than in NLE and the proportion of autoantibodies in dogs with NLE was low compared with those described for NME in previous reports [59, 90], it could be considered that these differences are related to the etiologies of the various conditions. In fact, in some previous reports [59, 81, 90, 92], the involvement of an autoantibody to astrocytes in the etiology of NME was indicated. However, double labeling IFA could not confirm whether these autoreactive inflammatory cells against GFAP are a primary cause or a secondary consequence of NME.

In some cases, malacic changes and inflammatory lesions were observed both in the gray matter and white matter in NME and NLE, although the distribution of lesions was different. The proportion of inflammatory cells was not significantly different. The presence of IgG in GFAP-positive astrocytes was observed in both NME and NLE. Thus, NME and NLE may be considered the same disease entity, necrotizing encephalitis, and divided into subtypes, the gray matter form and the white matter form, according to the distribution of lesions.

Although there have been many attempts to detect specific pathogens or

antigens that induce NME, NLE, or GME, all have failed except for the reports detailing the involvement of GFAP [11, 18, 19, 36, 55, 57, 59, 66, 69, 76, 78, 81, 84, 85, 88, 90, 91, 92, 93, 94]. Similarly, no specific pathogens or antigens have been detected in human multiple sclerosis (MS) [10, 42, 54, 64]. MS is an autoimmune-mediated, inflammatory, and demyelinating inflammatory disorder affecting the CNS white matter, which is divided into several subtypes according to the lesions produced and the clinical course of the disease. It is disputed whether MS is mediated by MHC class II-restricted CD4+ T cells, MHC class I-restricted CD8+ T cells, or antibody-complement complex [13, 38, 42, 48, 54, 52, 64, 73]. However, other evidence suggests that genetic factors such as HLA-DR2 play a crucial role in susceptibility to the familial type of MS [31, 32, 52, 64]. Chromosomes 17q22 and 6p21 (MHC) may also be associated with MS [31, 64, 75]. Taken together, multiple etiological factors including both environmental and genetic factors are likely to correlate with the onset of MS. In fact, it was reported that DLA-DR class II antigen may be associated with the cause of NME in pug dogs [30], and that the mutation of mitochondrial DNA is related to NLE in Yorkshire terriers [5]. Canine brain diseases might be caused by genetic and environmental factors as well as multiple immune-mediated mechanisms.

Table 1. Cases of NME, NLE, and GME

Case	Breed	Sex	Age	Clinical diagnosis
1	Pug	♂	3y5m	NME
2	Pug	♂×	2y2m	NME
3	Pug	♀	8y	NME
4	Pug	♀	7m	NME
5	Pug	♀	2y3m	NME
6	Pug	♂	6y	NME
7	Pug	♂	8m	NME
8	Pug	♀	7m	NME
9	Pug	♀	2y	NME
10	Pug	♂	1y2m	NME
11	Pug	♂	9m	NME
12	Pug	♀	1y	NME
13	Pug	unknown	unknown	NME
14	Maltese	♀	3y6m	NME
15	Maltese	♂	4y	NME
16	Papillon	♂	1y	NME
17	Papillon	♂	1y5m	NME
18	Pomeranian	♀	2y5m	NME
19	Pomeranian	♂	8y	NME
20	Shih-tzu	♀	13y	NME
21	Shih-tzu	♀	4y	NME
22	Chihuahua	♀	5y	NME
23	Chihuahua	♀	3y	NME
24	Miniature pinscher	♂	11y8m	NME
25	Toy poodle	♂	11y6m	NME
26	Yorkshire terrier	♀×	4y3m	NLE
27	Yorkshire terrier	♀	6y	NLE
28	Yorkshire terrier	unknown	unknown	NLE
29	Chihuahua	♂	unknown	NLE
30	Pug	♂	unknown	NLE
31	Miniature dachshund	♂	4y	GME
32	Miniature dachshund	♀	6y	GME
33	Beagle	♀	unknown	GME
34	Golden retriever	unknown	4y	GME
35	Toy poodle	♀	unknown	GME
36	Yorkshire terrier	♀×	4y	GME
37	Mixed	♀	6y	GME
38	Unknown	unknown	unknown	GME
39	Unknown	unknown	unknown	GME

Table 2. The primary antibodies used for IHC and double labeling IFA

Antibody (clone)	Manufacturer, country	Poly/mono	Dilution	Positive control	Result (in canine tissue)
CD163 (AM-3K)	Transgenic Inc., Japan	Mono-mouse anti-human	1:15~1:20	Macrophages	P (macrophages and a few microglia)
CD3	Dako, Japan	Poly-rabbit anti-human	1:20	T cells	P (T cells)
IgG	American Qualex, San Clemente, CA, U.S.A	Biotinylated sheep anti-canine IgG	1:100	Plasma cells	P (plasma cells and canine IgG)
CD79αcy	Dako, Japan	Mono-mouse anti-human	1:20	B cells and plasma cells	P (B cells and plasma cells)
CD20	Thermo Scientific, Fremont, CA	Poly-rabbit anti-human	1:400	B cells and a few T cells	P (B cells and a few T cells)
Myeloperoxidase	Dako, Japan	Poly-rabbit anti-human	1:300	Neutrophils and a few monoc	P (neutrophils)
Glial filament protein	PROGEN Biotechnik, Heidelberg, Germany	Mono-mouse anti-human	pre-diluted	Astrocytes	P (astrocytes)

P: positive, N: negative

Table 3. Distribution of lesions in NME, NLE, and GME

	NME	NLE	GME
Cerebral cortex	24/24 (100)	1/5 (20)	2/9 (22)
Cerebral white matter	12/24 (50)	5/5 (100)	8/9 (89)
Hippocampus	16/24 (67)	1/5 (20)	0/9 (0)
Thalamus	13/24 (54)	4/5 (80)	1/9 (11)
Midbrain	11/24 (46)	1/5 (20)	4/9 (44)
Cerebellum	7/24 (29)	1/5 (20)	8/9 (89)
Brain stem	1/24 (4)	1/5 (20)	4/9 (44)
Spinal cord	1/24 (4)	1/5 (20)	3/9 (33)

*Cases / Total (%)

Table 4. Histopathological comparison among NME, NLE, and GME

Pathological lesions		NME		NLE		GME	
		Distribution	Severity	Distribution	Severity	Distribution	Severity
	Malacic changes	Cerebral gray matter	Moderate to severe	Cerebral white matter, subcortical region	Moderate to severe	Not detected	
Ischemic neurons		Cerebrum, hippocampus	Moderate	Cerebrum, hippocampus	Mild	Cerebrum, hippocampus	Moderate
Inflammatory lesions	Perivascular cuff	Cerebral gray and white matters, cerebellum	Moderate to severe	Cerebral gray and white matters, cerebellum	Moderate to severe	Cerebral gray and white matters, cerebellum	Moderate to severe
	Parenchymal infiltration of inflammatory cells	Cerebral gray and white matters, cerebellum	Moderate to severe	Cerebral gray and white matters, cerebellum	Moderate to severe	Cerebral gray and white matters, cerebellum	Moderate to severe
	Subleptomeningeal infiltration	Meninges and sulcus	Moderate to severe	Meninges and sulcus, ependyma, and choroid plexus	Moderate to severe	Cerebellum, brain stem, and spinal cord	Moderate to severe
	Granulomatous lesions	Not detected		Not detected		Cerebellum, medulla oblongata, spinal cord, cerebral white matter, midbrain, thalamus, and hypothalamus	Severe
Glial reaction	Astrogliosis	Periphery of necrotic and inflammatory regions	Moderate to severe	Inflammatory regions of cerebral gray matter	Mild to moderate	Inflammatory regions of cerebral gray matter	Moderate to severe
	Microgliosis	Cerebral gray and white matters, cerebellum	Moderate to severe	Cerebral gray and white matters, cerebellum	Moderate	Cerebral gray and white matters, cerebellum	Moderate to severe
Vascular reaction		Cerebral gray and white matters, cerebellum	Moderate to severe	Cerebral gray and white matters, cerebellum	Moderate to severe	Cerebral gray and white matters, cerebellum	Moderate to severe

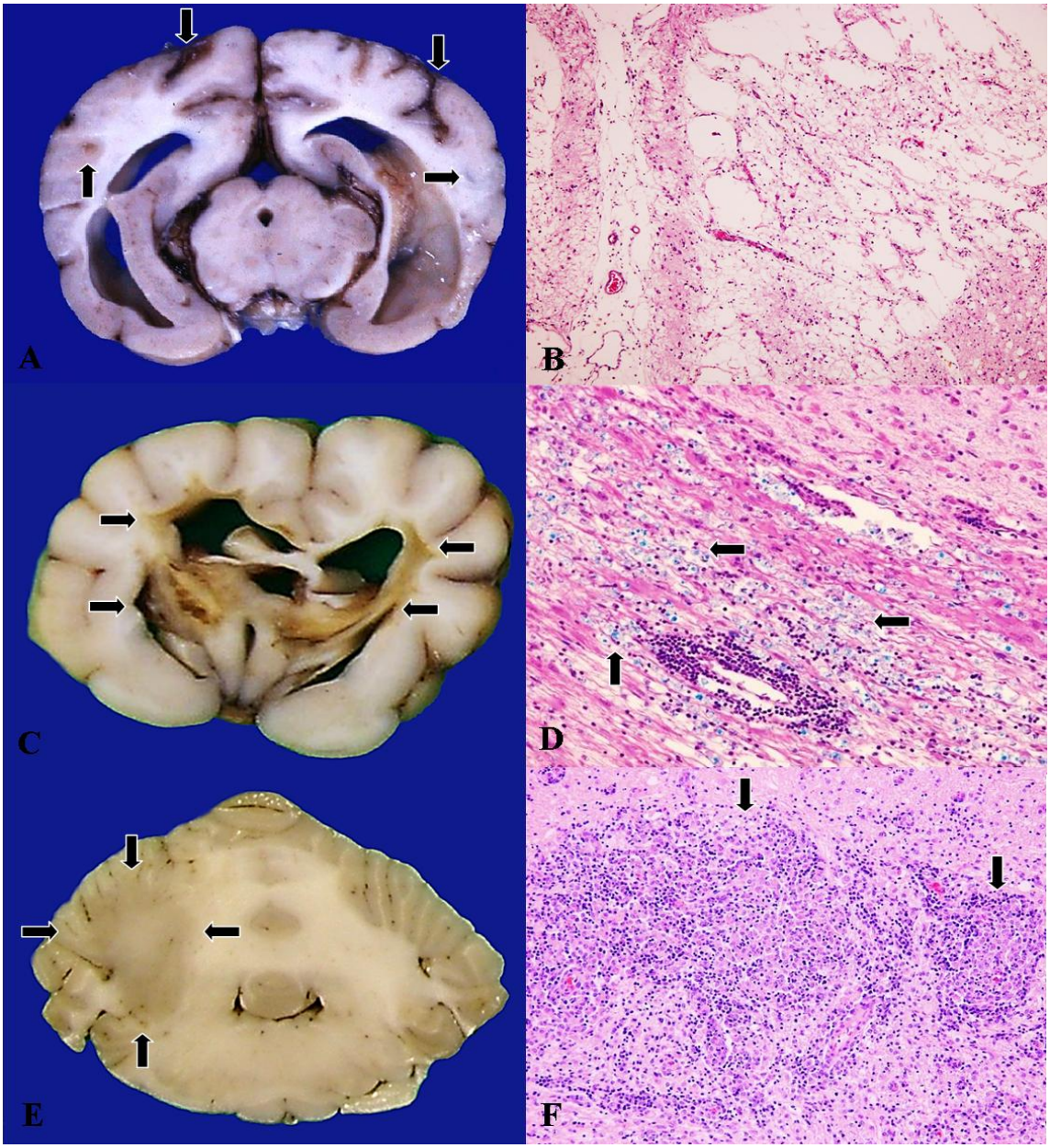

Figure 1. Histopathological lesions in NME, NLE and GME
(A, B) Cerebrum; pug, necrotizing meningoencephalitis (NME) (A) No. 5. Grey malacic changes (arrow) were observed in the cerebral cortex (ampullary sulcus, Sylvius sulcus). The lateral ventricles were dilated bilaterally. (B) No. 9. Malacic changes and infiltrating cells in the neuroparenchyma were observed in the cerebral cortex. HE. (C, D) Cerebrum; Yorkshire terrier, necrotizing leukoencephalitis (NLE), No. 27 (C) Yellowish malacic changes (arrow) were observed in the cerebral white matter (thalamus, internal capsule, and centrum semiovale). (D) Perivascular cuffs, and the parenchymal infiltration of inflammatory cells were observed in the cerebral white matter. Demyelinations was characterized by the prominent infiltration of lipid-laden (blue) macrophages (arrow) in the cerebral white matter, and astrocytosis in the cerebral subcortex. LFB-HE. (E, F) Cerebellum; beagle, granulomatous meningoencephalomyelitis (GME), No. 33. (E) Grey areas (arrow) were found in the cerebellar white matter. (F) Granulomatous lesions (arrow), perivascular cuffs, and areas of parenchymal infiltration were prominent in the cerebellar white matter. HE.

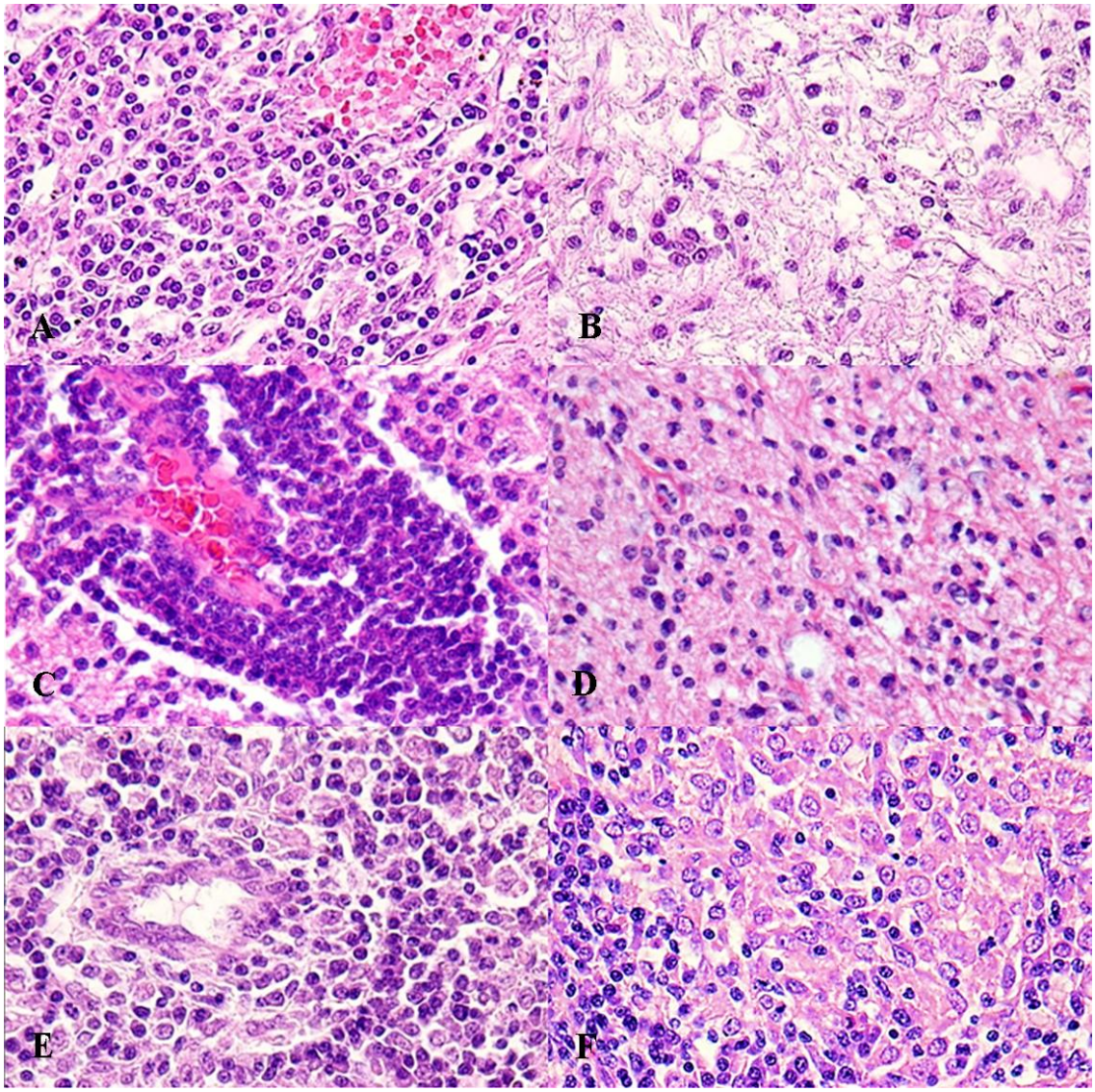

Figure 2. Characterisitic inflammatory lesions in NME, NLE and GME
(A, B) Cerebrum; pug, NME, No. 5. (A) Perivascular cuffs, composed of plasma cells and lymphocytes, were found in the cerebral cortex and subcortex. HE. (B) Infiltration of inflammatory cells, such as plasma cells and lymphocytes, were observed in the cerebral cortex and subcortex. HE. (C, D) Cerebrum; Yorkshire terrier, NLE, No. 27. (C) Perivascular cuffs were observed in the cerebral white matter and parts of the subcortex. HE. (D) Infiltration of inflammatory cells and microgliosis were found in the cerebral white matter and parts of the subcortex. HE. (E, F) GME (E) Cerebellum; Beagle, No. 33. Perivascular cuffs, composed of macrophages, lymphocytes, and plasma cells, were found in the cerebellar white matter. HE. (F) Cerebrum; toy poodle, No. 35. Characteristic nests of epithelioid cells were found in the cerebellar white matter. HE.

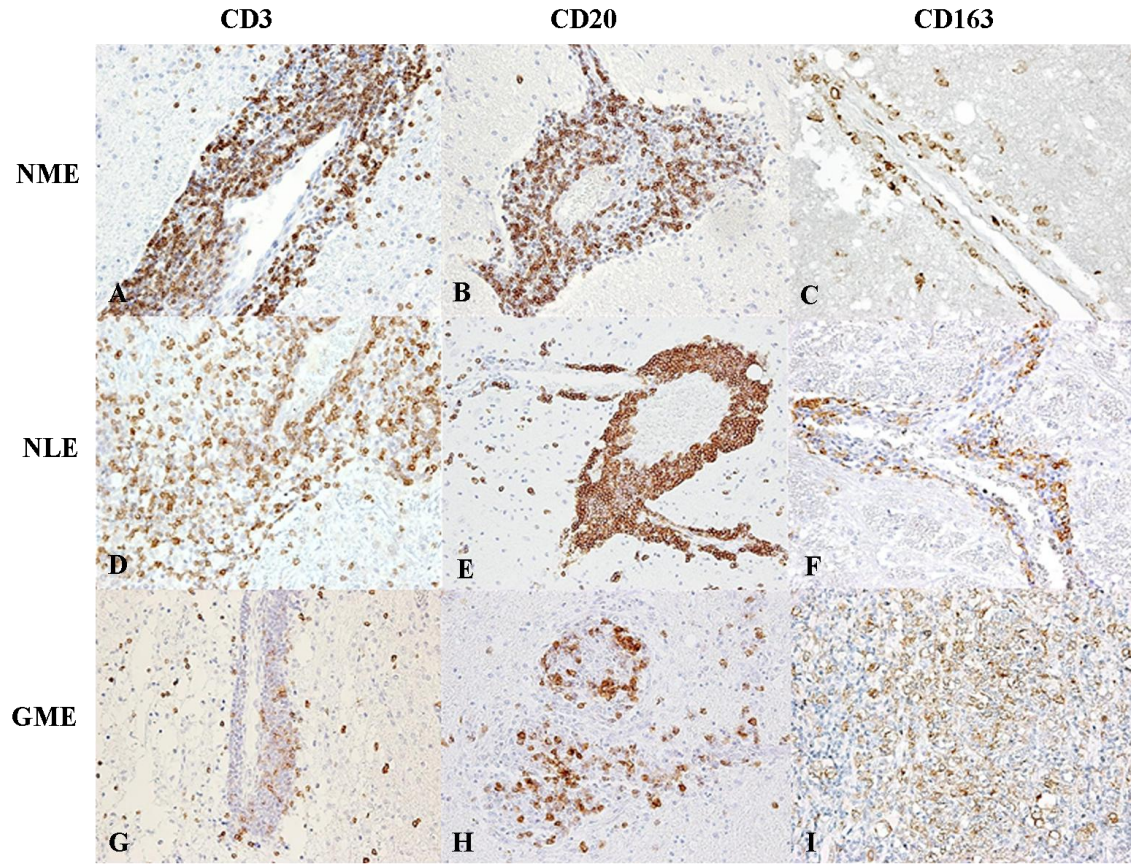

Figure. 3 Immunohistochemistries on NME, NLE and GME
(A~C) Cerebrum; pug, NME, No. 1. (A) CD3-positive T cells were observed in the Virchow-Robin space (perivascular cuffs) and the neuroparenchyma. (B) Large numbers of CD20-positive B cells were observed in the Virchow-Robin space (perivascular cuffs). (C) CD163-positive macrophages were observed in the perivascular cuffs as well as malacic neuroparenchyma. (D~F) Cerebrum; Yorkshire terrier, NLE, No. 26. (D) CD3-positive T cells were observed in the Virchow-Robin space (perivascular cuffs) and the neuroparenchyma. (E) CD20-positive B cells were observed in the Virchow-Robin space (perivascular cuffs) prominently. (F) CD163-positive macrophages were observed in the perivascular cuffs. (G~I) Cerebellum; beagle, GME, No. 33. (G) CD3-positive T cells were present in the Virchow-Robin space (perivascular cuffs). (H) CD20-positive B cells were observed in the perivascular cuffs as well as the neuroparenchyma in proximity to the nest of epithelioid cells. (I) Characteristic nest of epithelioid cells, CD163-positive, were observed in the neuroparenchyma.

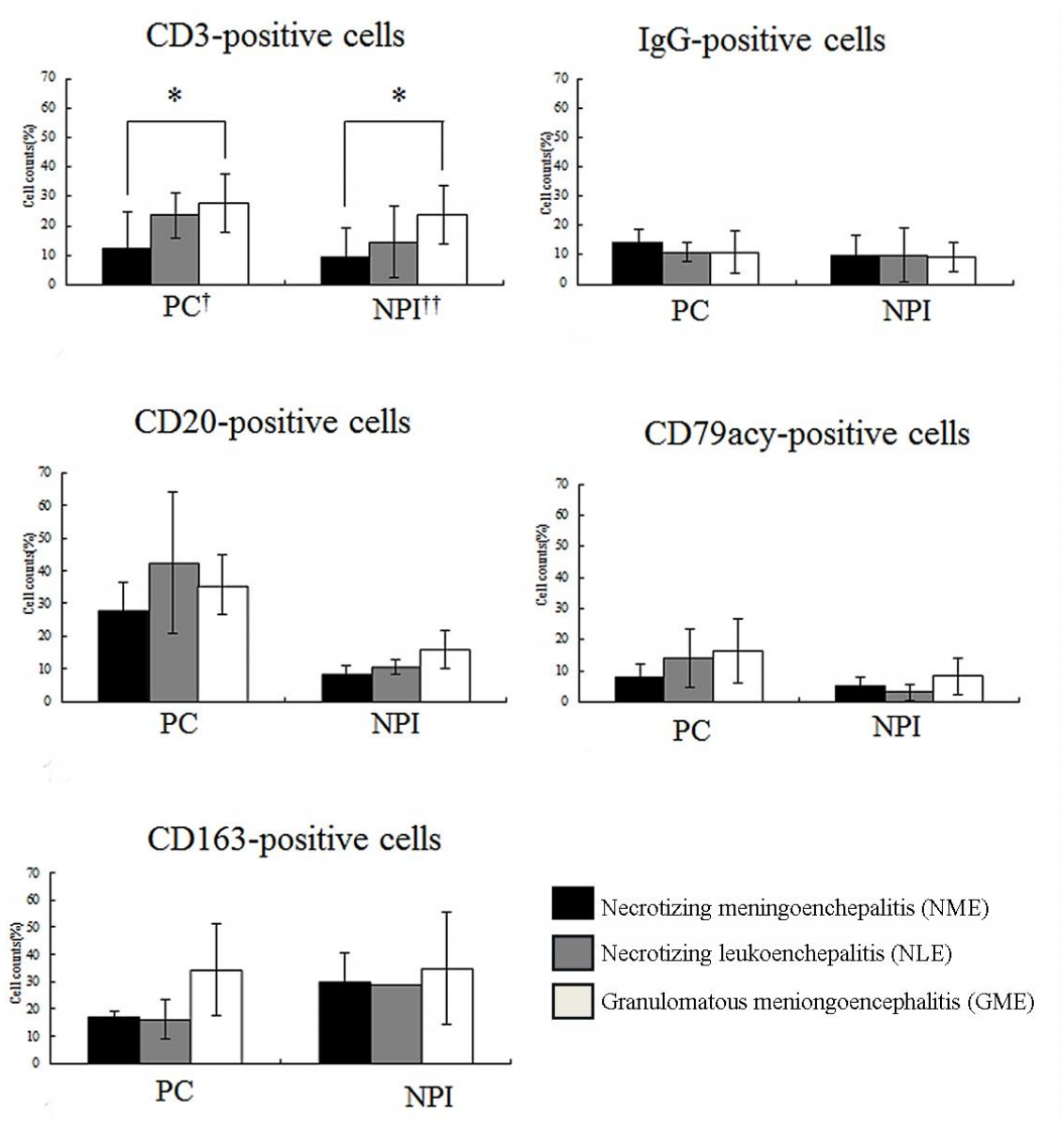

Figure 4. The percentages of CD3-, IgG-, CD20-, CD79acy-, and CD163-positive cells (mean±SEM, %) in the perivascular cuffs (PC) and neuroparenchymal infiltration (NPI) in animals with NME, NLE, and GME (*$P<0.01$).

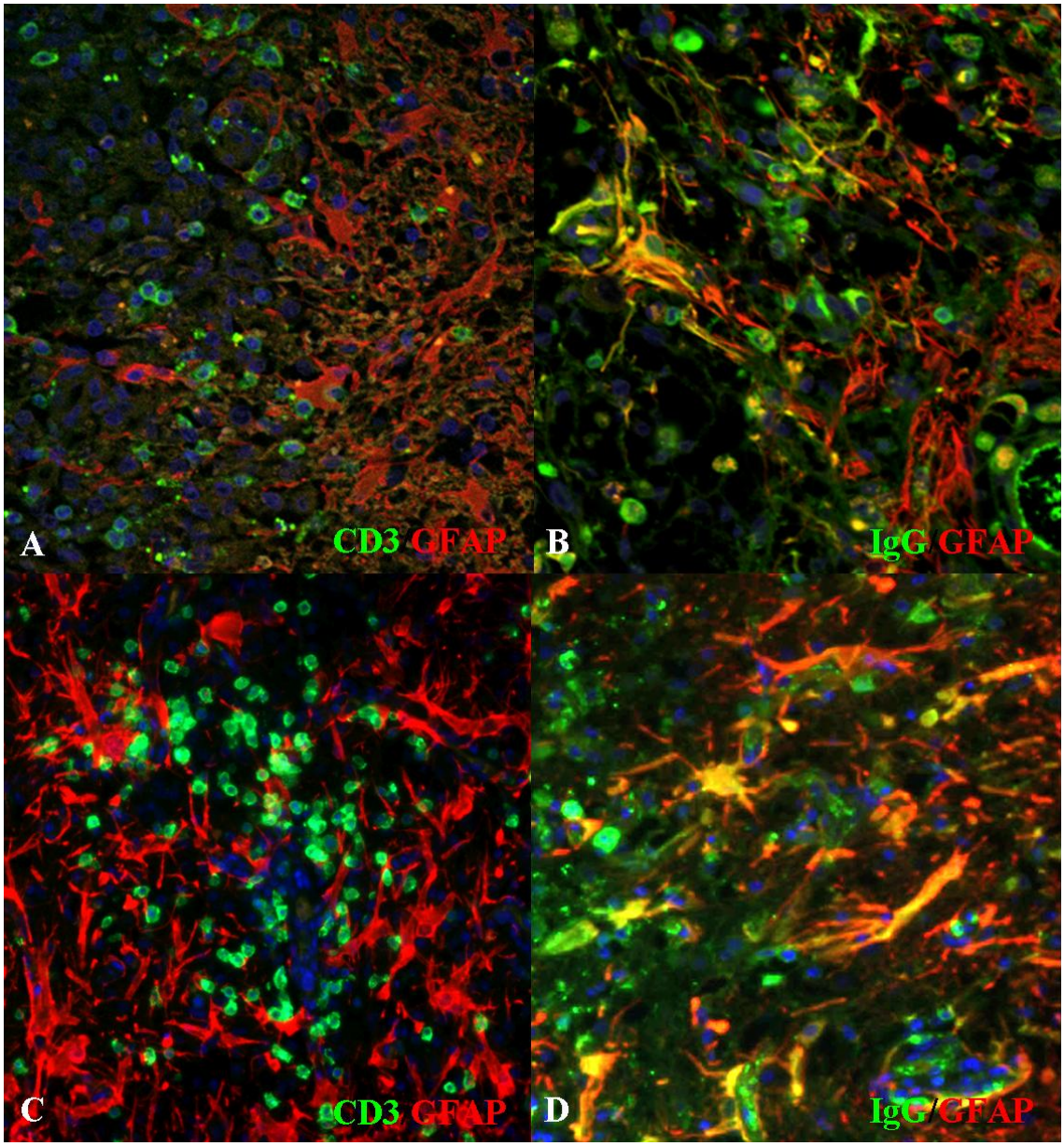

Figure 5. Double-labeling stains in NME, NLE and GME
(A, B) Cerebrum; papillon, NME, No. 17. (A) CD3-positive T cells are represented as green signals produced by FITC, and GFAP-positive astrocytes are represented as red signals produced by Alexa 594. Nuclei are represented as blue signals produced by DAPI. Many CD3-positive T cells (green) were in close proximity to GFAP-positive astrocytes (red) in the peripheral malacic regions of the cortex. (B) Ig G and IgG-positive plasma cells are represented as green signals produced by FI TC, and GFAP-positive astrocytes are represented as red signals produced by Ale xa 594. Nuclei are represented as blue signals produced by DAPI. The cytoplasm and/or processes of some astrocytes were labeled with both IgG and GFAP (yellow) in NME. These double-positive astrocytes were more prominent in NME than NLE. (C, D) Cerebrum; Yorkshire terrier, NLE, No. 27. (C) In the NLE, CD3-positive T cells had infiltrated among the fibrous processes of GFAP-positive astrocytes in the white matter. (D) The cytoplasm and/or processes of some astrocytes were labeled with both IgG and GFAP (yellow) in NLE.

Chapter II

Th1-, Th2- and Th17-related cytokine and chemokine receptor mRNA and protein expression in brain tissues, T cells and macrophages in dogs with necrotizing and granulomatous meningoencephalitis

Summary

Necrotizing meningoencephalitis (NME), necrotizing leukoencephalitis (NLE) and granulomatous meningoencephalomyelitis (GME) are idiopathic inflammatory diseases in the central nervous system (CNS) of dogs. In our previous study, the proportion of inflammatory cells, except the CD3-positive T cells, in parenchymal and perivascular lesions in the brain did not differ. However the breed-specificities, clinical courses and specific lesions were distinct among these diseases. Thus, similarities and differences of the pathology among these diseases were implied. In this study, mRNA and/or protein expression levels of cytokines and chemokine receptors were investigated in NME (n=2), NLE (n=4), and GME (n=2) cases, and their relationship in the formation of specific lesions was discussed. The mRNA and protein expression levels of IFN-γ and IL-17 were marked in NME and GME, respectively. Also, mRNA expression levels of CXCR3 and CCR2 were prominent in NME and GME, respectively. Results of double-labeling immunofluorescence to identify cells producing IL-17 in these lesions showed that most CD163-positive macrophages/microglia, but fewer CD3-positive T cells, were IL-17-positive in GME. From these results, it seems that IFN-γ play key roles in the lesions of NME, and macrophages/microglia that infiltrate brain lesions producing IL-17 are more important in GME than T cells.

Introduction

Necrotizing meningoencephalitis (NE) and granulomatous meningoencephalomyelitis (GME) are idiopathic inflammatory diseases in the central nervous system (CNS) of dogs. NE is characterized by malacic changes and is subdivided into necrotizing meningoencephalitis (NME, the gray matter type) and necrotizing leukoencephalitis (NLE, the white matter type) according to the location of lesions. NE appears to be breed-specific and affects the pug [11, 19, 47, 55], shi-tzu [88], papillon [88], maltese [26, 68, 85], Chihuahua [34], yorkshire terrier [5, 24, 50, 57, 91, 93], and french bulldog [84]. Conversely, GME is characterized by granulomatous lesions in the cerebral white matter and cerebellum and is not breed-specific. While the cause of these diseases still remains obscure, it has been reported that CD3-positive T cells play significant roles [43, 88, 89]. Also, in our previous report [chapter 1], CD3-positive T cells were the most prominent inflammatory cells in these diseases, especially in GME lesions. CD163-positive macrophages were more predominant in GME than in NME and NLE, although this was not significant. The proportion of IgG-, CD20-, CD79acy-, and myeloperoxidase-positive inflammatory cells was not different among these diseases. Overall, the proportion of inflammatory cells in parenchymal and perivascular lesions in the brain does not greatly vary among these diseases, although marked differences in the histopathology of lesions and their location have been observed. Thus, we concluded that these diseases may share a common pathogenesis.

It has been assumed that Th1 cells mediate human autoimmune diseases, such as multiple sclerosis (MS) [53, 83, 95] and rheumatoid arthritis (RA) [17, 77]. In murine experimental autoimmune encephalitis (EAE), a disease model of MS, similar phenomena have also been recognized [4, 95]. However, treatment with an antagonist

of Th1 cells could not prevent and/or ameliorate the symptoms of MS and EAE [4, 7, 53]. Also, it was suspected that humoral immunity, especially B cells, may mediate these diseases [48]. It was then discovered that Th17 cells play a key role in MS and EAE [4, 40] and that self-specific Th17 cells are highly pathogenic in autoimmune diseases such as RA [37, 49, 80], autoimmune uveitis [96], and Crohn's disease [12, 46]. It has been suggested that Th17 cells are important at the initiation of such diseases and that Th1 cells are also important for the maintenance and/or deterioration of these diseases [4, 71].

Chemokine receptors, such as chemokine (C-X-C motif) receptor 3 (CXCR3), C-C chemokine receptor type 2 (CCR2), and C-C chemokine receptor type 4 (CCR4), have also been reported to be associated with MS and EAE [4]. CXCR3 is expressed primarily on activated T cells, such as Th1 cells [3, 15]. Th1 cells that express CXCR3 produce a large amount of IFN-γ [4, 15]. It has also been reported that T cells expressing CCR2 produce a large amount of IL-17 [3, 4, 74]. CCR4 is expressed on leukocytes [3, 4, 15, 74]. T cells that express CCR4 produce IL-4 or IL-17 according to the co-expression of CRTh2 or CCR6 [3, 4, 15, 74].

In the present study, we compared the levels of inflammatory cytokines and chemokine receptors in the brain lesions of NME, NLE, and GME cases, and discussed the relationship of these cytokines in the formation of specific lesions.

Materials and Methods

Brain tissues

Frozen brain tissues from NME (n=2), NLE (n=4), GME (n=2), and control (n=3) cases were used in this study (Table 1). NME, NLE and GME were diagnosed by histopathological examination. Potential infectious causes were excluded by both

histopathological examination and immunohistochemistry against canine distemper virus (CDV).

RNA extraction and cDNA synthesis

Total RNA was prepared by the guanidinium thiocyanate-phenol-chloroform method (ISOGEN, Wako, Osaka, Japan) from brain tissues and reverse-transcribed with a PrimeScript® RT-PCR kit (Takara, Otsu, Japan).

Real-time PCR quantification using SYBR Green I

Real-time PCR on the ABI PRISM (Applied Biosystems, Foster City, CA, USA) was performed in a total volume of 25μl of SYBR® Green Realtime PCR Master Mix (TOYOBO, Osaka, Japan) and primers for either CCR2, CCR4, CXCR3, GAPDH, IFN-γ, IL-12p35, IL-12p40, TBX21, IL-4, IL-10, GATA3, IL-17, IL-21, or RORγt (Table 2). The PCR reaction was performed on a MicroAmp™ Optical 96-well Reaction Plate (Applied Biosystems) with an initial degeneration step at 54°C for 30s and at 95°C for 3m, followed by 10 cycles at 95°C for 30s, and an annealing step at 68°C for 1m, at 72°C for 30s, and 30 cycles at 95°C for 30s. At the end of each cycle, the intensity of fluorescence emitted from SYBR Green was measured. After completion of the process, samples were subjected to a dissociation curve analysis (from 60°C above annealing temperature to 95°C). Samples were then quantified automatically (7900HT version 2.3 Sequence Detection Systems, Applied Biosystems). A single narrow peak was observed by the dissociation curve analysis at the specific melting temperature and a single band of the predicted size was observed by 2% agarose gel electrophoresis. Each case was compared with a control group by the ΔΔCt method and relative quantification was performed.

Immunoblot

Brain tissues from NME, NLE, and GME cases were homogenized with a TissueRuptor (QIAGEN, Homebrechtikon, Switzerland) and TissueRuptor disposable probes (QIAGEN) in a buffer containing 10mM Tris-HCl (pH 7.8), 1% NP-40, 0.1% SDS, 150mM NaCl, 1mM EDTA (pH 8.0), Proteinase inhibitor cocktail, 2mM Na_3VO_4, 10mM NaF, and DW. Lysates were incubated on ice for 30 min and centrifuged at 12000g at 4°C for 20 min. Supernatants were collected. Proteins were separated by SDS-PAGE and were transferred to Immun-Blot® PVDF Membranes (BIO-RAD, Hercules, CA, USA). Membranes were blocked with 150 mM NaCl, 10 mM Tris-Base, and 40 mM Tris-HCl buffer (pH 7.8) containing 5% skim milk and 0.05% Tween-20 and were incubated with one of the primary antibodies at 4°C overnight and then with appropriate secondary antibodies at room temperature for 1 hour. The primary antibodies used were listed in Table 3 and the secondary antibodies were donkey anti-goat IgG horseradish (HRP)-conjugated (1:5000, Santa Cruz Biotechnology, Santa Cruz, CA, USA) and donkey anti-rabbit IgG HRP-conjugated (1:5000, GE Healthcare, Buckinghamshire, UK). Membranes were visualized with Amersham ECL Prime Western blotting detection reagent (GE Healthcare, Uppsala, Sweden) using a Molecular Imager® ChemiDox™ XRS+ with Image Lab™ software (BIO-RAD, Tokyo, Japan). Positive bands were relatively quantified using Image Lab™ software (BIO-RAD) compared to a beta-actin band.

Double-labeling Immunofluorescence quantification

Ten μm thick-OCT compound-embedded frozen brain tissue sections were first treated with skimmed milk at 37°C for 40 min. Sections were then incubated at 4°C overnight with a first primary antibody and then with a second primary antibody at

37°C for 1 hour. Primary antibodies used were listed in Table 3. A secondary antibody cocktail was employed at room temperature for 1 hour. The cocktail included fluorescein isothiocyanate-labeled horse anti-mouse IgG (1:200, Vector Laboratories, Burlingame, CA, USA) and Alexa fluor 594-labeled donkey anti-rabbit IgG (1:200, Invitrogen, Eugene, OR, USA). Sections were finally mounted with Vectashield HardSet with DAPI (Vector Laboratories) and observed using a Leica DMI3000 B fluorescence microscope. The number of positive cells was counted under x 400 magnification in 5 to 10 selected fields, perivascular cuffs or neuroparenchymal infiltrates, of each case and the mean percentage was calculated.

Results

mRNA levels of cytokines and transcription factors

Among cytokines for the Th1 immune response, IFN-γ mRNA levels in the two NME cases were markedly higher than those in NLE and GME cases. IL-12B mRNA levels were high in the two GME cases, and moderately high in the one NLE case (Fig. 1, *upper*). However, the expression levels of a Th1 cytokine, IL-12A, and the transcription factor, TBX21, were not different between the diseases (Fig. 1, *upper*). Among the cytokines for the Th2 immune response, IL-4 mRNA levels were high in NLE and GME cases (Fig. 1, *middle*). However, IL-10 levels were not different between the diseases, although that was moderately high in the one NME case (Fig. 1, *middle*). GATA3 levels, a transcription factor of Th2 cells, were high in all NME and GME cases, and one NLE case, but not in the other three NLE cases (Fig. 1, *middle*). In cytokines of the Th17 immune response, IL-17 as well as IL-21 mRNA levels were the highest in GME cases, and considerable in the one NLE case (Fig. 1, *bottom*). RORγt levels, a transcription factor of Th17 cells, were moderate and similar between

the diseases (Fig. 1, *bottom*). IL-12B is a subunit of IL-23, a stimulating factor of the secretion of IL-17, as well as IL-12. Thus, the high expression level of IL-12B in GME cases signifies that the Th17 immune response is more connected than the Th1 immune response. Conclusively, IFN-γ was prominent in NME, and IL-17 and IL-21 were marked in GME.

mRNA levels of chemokine receptors

Among chemokine receptors, CXCR3, CCR2, and CCR4 mRNA levels were examined. In NME and NLE cases, CXCR3 mRNA levels were the highest among the three chemokine receptors (Fig. 2). CCR2 and CCR4 mRNA levels were similar in NME and NLE cases (Fig. 2). In GME cases, CCR2 mRNA levels were the highest among the three chemokine receptors, though the levels in all three were similar (Fig. 2). Also, CCR2 mRNA levels in GME cases were higher than those in NME and NLE cases (Fig. 2). These results imply that cells expressing CXCR3, such as Th1 cells and macrophages/microglia, infiltrated in NME or NLE cases and cells expressing CCR2, such as Th17 cells and macrophages/microglia, infiltrated prominently in GME cases.

Protein levels of cytokines

To confirm whether protein expressions of cytokines in brain lesions were similar to those of mRNA, we measured expression levels by immunoblot analysis. Expression of the IFN-γ protein was high in NME cases, which reflected mRNA expression results (Fig. 3, *upper*). IL-4 was expressed prominently in one NLE case (No. 5) (Fig. 3, *middle*). IL-17 was expressed prominently in two GME cases (Fig. 3, *bottom*). Transcription factors were expressed similarly in all cases and controls, except for the expression of the RORγt protein, which appeared slightly higher in NME

and GME (data not shown). Conclusively, predominant cytokines were distinct in diseased tissues among these diseases, as IFN-γ and IL-17 were expressed predominantly in NME and GME, respectively.

IL-17 and IL-17-producing and/or secreting inflammatory cells

To identify cells that produce IL-17 in brain lesions, we performed double-labeling immunofluorescence. It seemed that CD163-positive macrophages/microglia were more positive for IL-17 than CD3-positive T cells. Indeed, CD163-positive macrophages/microglia prominently infiltrated GME, NME, and NLE brains in this order. The percentage of IL-17-positive cells in CD163-positive macrophages/microglia was the highest in GME cases, which were 46% (No. 6) and 73% (No. 7) (Fig. 4, *upper*). CD3-positive T cells infiltrated in GME and NME cases, and less in NLE cases (Fig. 4, *middle*). The percentage of IL-17-positive cells in CD3-positive T cells was higher in GME cases, which were 20% (No. 6) and 28% (No. 7). HLA-DR-positive APCs predominantly infiltrated NME and GME brains, and 35% (No. 6) and 32% (No. 7) of them were IL-17-positive in GME (Fig. 4, *bottom*). We then performed double-labeling immunofluorescence against HLA-DR for APCs such as macrophages, B cells and dendritic cells. Since CD20-positive B cells were not predominant among these diseases and were negative for IL-17, the result of double-labeling immunofluorescence against HLA-DR and IL-17 reinforced that against CD163 and IL-17. Conclusively, these results showed that macrophages/microglia which infiltrate brain lesions produce IL-17 more than T cells do.

Discussion

In the present study, the cytokine profile in brain lesions was characteristic of

each lesion in NME, NLE, and GME. Expression levels of IFN-γ and IL-17 were prominent in NME and GME cases, respectively. For chemokine receptors, expression levels of CXCR3 and CCR2 were the most prominent in NME and GME cases, respectively. Given that T cells and/or macrophages/microglia expressing CXCR3 or CCR2 have been reported to produce a large amount of IFN-γ or IL-17, respectively, these results were consistent with the results of cytokines [3, 4, 15, 74].

It is evident that NME and NLE could be associated with autoimmunity against GFAP [chapter 1, 59, 81, 92]. Autoreactive T cells, B cells, and autoantibodies against astrocytes were identified in these diseases [chapter 1]. CD3-positive T cells, CD20-positive B cells, IgG-positive plasma cells, and HLA-DR-positive or CD163-positive microglia or macrophages accumulated in these lesions [chapter 1]. In this report, lesions such as perivascular cuffs and the infiltration of inflammatory cells in the neuroparenchyma were also prominently observed among the three diseases studied. It has been reported that IFN-γ predominated in the perivascular cuffs of active MS lesions [65, 95]. IFN-γ has cytotoxic characteristics [65, 95] and malacic changes were prominent in NME cases of this report. Therefore, such high expression levels of IFN-γ could be associated with inflammatory lesions in NME cases. A previous study has suggested that astrocytes stimulate the secretion of IFN-γ and IL-17 from T cells and macrophages through the secretion of IL-23 [62]. The possibility cannot be excluded that the low expression of IL-17 in NME and NLE in the present results might be due to astrocyte damages. However, considering that CXCR3 mRNA expression levels involved in the secretion of IFN-γ were prominent in NME cases, IFN-γ is thought to be important in NME.

In the one NLE case, the mRNA expression profile was similar to those of GME and NME cases, which showed high IL-4, IL-17 and IL-21 in cytokines same as

those in GME cases, and high CXCR3 in chemokine receptors same as in NME cases. However, in the protein expression level, only IL-4 was marked. Since the other three NLE cases in this report included more lesions of the end phase, differences in the cytokine repertoire between NLE cases could be accounted for. We observed a few cases that had general inflammatory lesions, but not distinct lesions or showed intermixed distinct lesions and distributions among the three diseases. Thus, differential diagnoses had to be considered. This one NLE case could be one of those cases and not a typical NLE case. In fact, this case showed distinct malacic changes in the cerebral white matter, and the distribution was similar to that of GME. As a result, although the IL-4 expression level in this one NLE case was distinct, how important IL-4 is in NLE cases is not clear.

mRNA expression levels of IL-17, CCR2, or CCR4, which are involved in the secretion of IL-17, and protein expression levels of IL-17 [3, 4, 15, 74], were higher in GME cases than in NME and NLE cases. We then performed double staining to confirm which inflammatory cells produce IL-17. It had been expected that most CD3-positive cells produce IL-17 since they infiltrated GME lesions the most markedly [chapter 1]. However, a large number of CD163-positive cells were also positive for IL-17 in the present GME cases. The number of CD3- and IL-17-double positive cells was modest. Some HLA-DR-positive cells were IL-17-positive in GME. Therefore, mainly CD163-positive cells may produce IL-17 in GME.

It has been reported that IL-17 is involved in autoimmune diseases, allergic reactions, and anti-tumor immunities, and that infiltrating Th17 cells produce IL-17 in some autoimmune diseases, such as rheumatoid arthritis [37, 39, 80], Crohn’s disease [12, 46], MS, and EAE [4, 20, 40, 71]. Neutrophils, eosinophils, mast cells, and macrophages also produce IL-17 in the lesions of allergic reactions [65, 82]. It has

been suggested that GME is related to delayed-type hypersensitivity [43, 89]. Mast cells may also participate in the acute phase lesions of GME and stimulate the development of GME lesions by increasing the permeability of the blood-brain barrier (BBB) [23]. Neutrophils included in the granulomatous lesions of GME as well as mast cells may be involved in IL-17 production directly or indirectly through macrophages [23]. Taken together, IL-17 being produced by macrophages may be an important factor for the formation of GME lesions.

The present study is the first to analyze the expression levels of cytokines in canine NME, NLE, and GME. From the results, it is thought that the pattern of mRNA and protein expression of cytokine and chemokine receptor would be distinctly different in diseased tissues and inflammatory cells in necrotizing and granulomatous forms of immune brain disease in small breeds; IFN-γ and CXCR3 in NME, IL-17 and CCR2 in GME. This could be associated with the pathological characteristics of each disease, despite the limitation of the small sample of fresh tissue available. Furthermore, macrophages within inflamed brain tissue appear to be disproportionately involved with IL-17 production compared to CD3-positive T cells in GME.

Table 1. Cases of canine NME, NLE, and GME examined

Case number	Breed	Sex	Age	Clinical diagnosis
1	Pug	F	2y6m	NME
2	Pug	F	2y10m	NME
3	Chihuahua	M	8y11m	NLE
4	Chihuahua	M	5y6m	NLE
5	Chihuahua	F	5y	NLE
6	French bulldog	F	2y11m	NLE
7	Miniature Dachshund	M	4y	GME
8	Beagle	F	Unknown	GME
9	Beagle	M	1y8m	Control
10	Beagle	M	1y8m	Control
11	Beagle	M	1y9m	Control

Table 2. Primers used for real-time RT-PCR

Gene	Accession No.	Direction	Nucleotide sequence	Annealing temperature	Product size
GAPDH	XM 003434387	forward	GGAGAAAGCTGCCAAATATG		194bp
		reverse	ACCAGGAAATGAGCTTGACA		
IFN-γ	AF126247.1	forward	TCAAGGAAGACATGCTTGGCAAGTT	68℃→ 58℃	98bp
		reverse	GACCTGCAGATCGTTCACAGGAAT		
IL-12A p35	NM 001003293.1	forward	TGCCTGGCCTCTGGAAAG	68℃→60℃	74bp
		reverse	TACATCTTCAAGTCCTCAT		
IL-12B p40	NM 001003292.1	forward	GCCAAGGTCGTGTGCCA	68℃→60℃	81bp
		reverse	CCAGTCGCTCCAGGATGAAC		
IL-4	AF187322.1	forward	TCACCAGCACCTTTGTCCACGG	64℃	96bp
		reverse	TGCACGAGTCGTTTCTCGCTGT		
IL-10	NM 0010030771.	forward	CAGGTGAAGAGCGCATTTAGT	68℃→60℃	107bp
		reverse	TCAAACTCACTCATGGCTTTGT		
IL-17	NM 001165878.1	forward	CACTCCTTCCGGCTAGAGAA	68℃→60℃	71bp
		reverse	CACATGGCGAACAATAGGG		
IL-21	NM 001003347.1	forward	GCCCATAAATCAAGCTTCCA	68℃→60℃	126bp
		reverse	TTCTGGAGCTGGCAGAGATT		
TBX21	XM 548164.2	forward	AAGCAGGGGCGGCGGATGTT	68℃→60℃	135bp
		reverse	ACTGCACCCACTTGCCGCTC		
GATA3	XM 844060.1	forward	CGAAGGCTGTCGGCAGCAAGAA	68℃→60℃	98bp
		reverse	ACGGGGTCTCCGTTGGCATT		
RORγt	XM 540323.3	forward	TCAACGCCAACCGTCCGGG	68℃→60℃	143bp
		reverse	CCGAAGCTTCCCCTTGGGCG		
CCR2	XM 541906.1	forward	ACATGCTGTCCACATCGCA	66℃→60℃	91bp
		reverse	GGCGCGCTGTAATCATAGTC		
CCR4	NM 001003020.1	forward	CGAGCGCAACCATACCTACT	66℃→60℃	200bp
		reverse	CGGCAAAGACCATCCTCACT		
CXCR3	NM 001011887.1	forward	TGGATGTGGCCAAGTCTGTC	68℃→60℃	200bp
		reverse	TGAGGGGGTCTCGGACCAG		

Table 3. Primary antibodies used for immunoblot analysis and double-labeling immunofluorescence

Antibody	Manufacturer	Poly/mono	Dilution	Application
β-actin	Cell Signaling Technology, Danvers, MA	Poly-rabbit anti-human	1:2000	IB*
IFN-γ	R&D Systems, Minneapolis, MN	Poly-goat anti-canine	1:1000	IB
IL-4	R&D Systems, Minneapolis, MN	Poly-goat anti-canine	1:500	IB
IL-17	Abcam, Tokyo, Japan	Poly-rabbit anti-human	1:1000, 1:50	IB, IF(d)**
GATA3	Abcam, Tokyo, Japan	Poly-rabbit anti-human	1:500	IB
RORγt	Abcam, Tokyo, Japan	Poly-goat anti-human	1:2000	IB
T-bet	Invitrogen, Camarillo, CA	Mono-rabbit anti-human	1:100	IB
CD3	Dako, Kyoto, Japan	Mono-mouse anti-human	1:10	IF(d)
CD163	Transgenic, Kumamoto, Japan	Mono-mouse anti-human	1:50	IF(d)
HLA-DR	Dako, Kyoto, Japan	Mono-mouse anti-human	1:100	IF(d)

* : Immunoblot, ** : Immunofluorescence (Double-labeling)

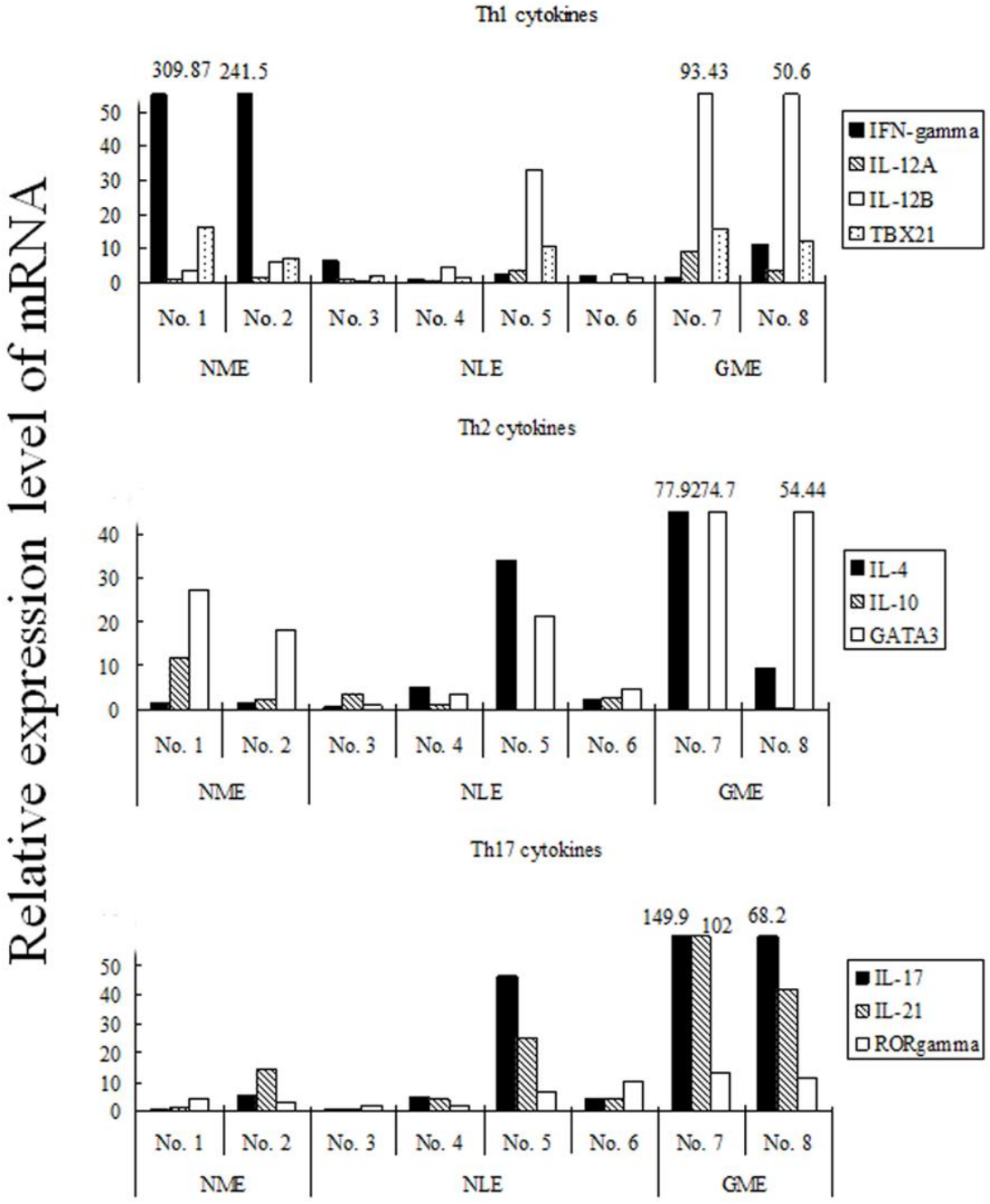

Figure. 1. mRNA levels of cytokines by real-time quantitative RT-PCR.
The relative mRNA level of each cytokine relative to controls was measured and calculated in NME (No. 1 and No. 2), NLE (No. 3, No. 4, No. 5, and No. 6), and GME (No. 7 and No. 8). (upper) Th1 cytokines, IFN-γ, IL-12A, and IL-12B, and the transcription factor, TBX21. (middle) Th2 cytokines, IL-4 and IL-10, and the transcription factor, GATA3. (bottom) Th17 cytokines, IL-17 and IL-21, and the transcription factor, RORγt.

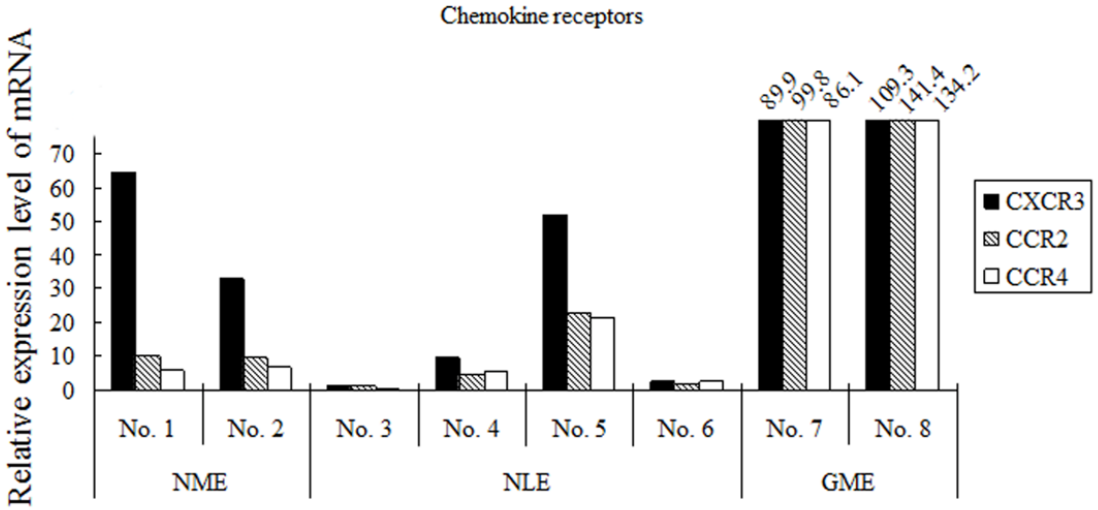

Figure. 2. mRNA levels of chemokine receptors by real-time quantitative RT-PCR. The relative mRNA level of each chemokine receptor relative to controls was measured and calculated in NME (No. 1 and No. 2), NLE (No. 3, No. 4, No. 5, and No. 6), and GME (No. 7 and No. 8).

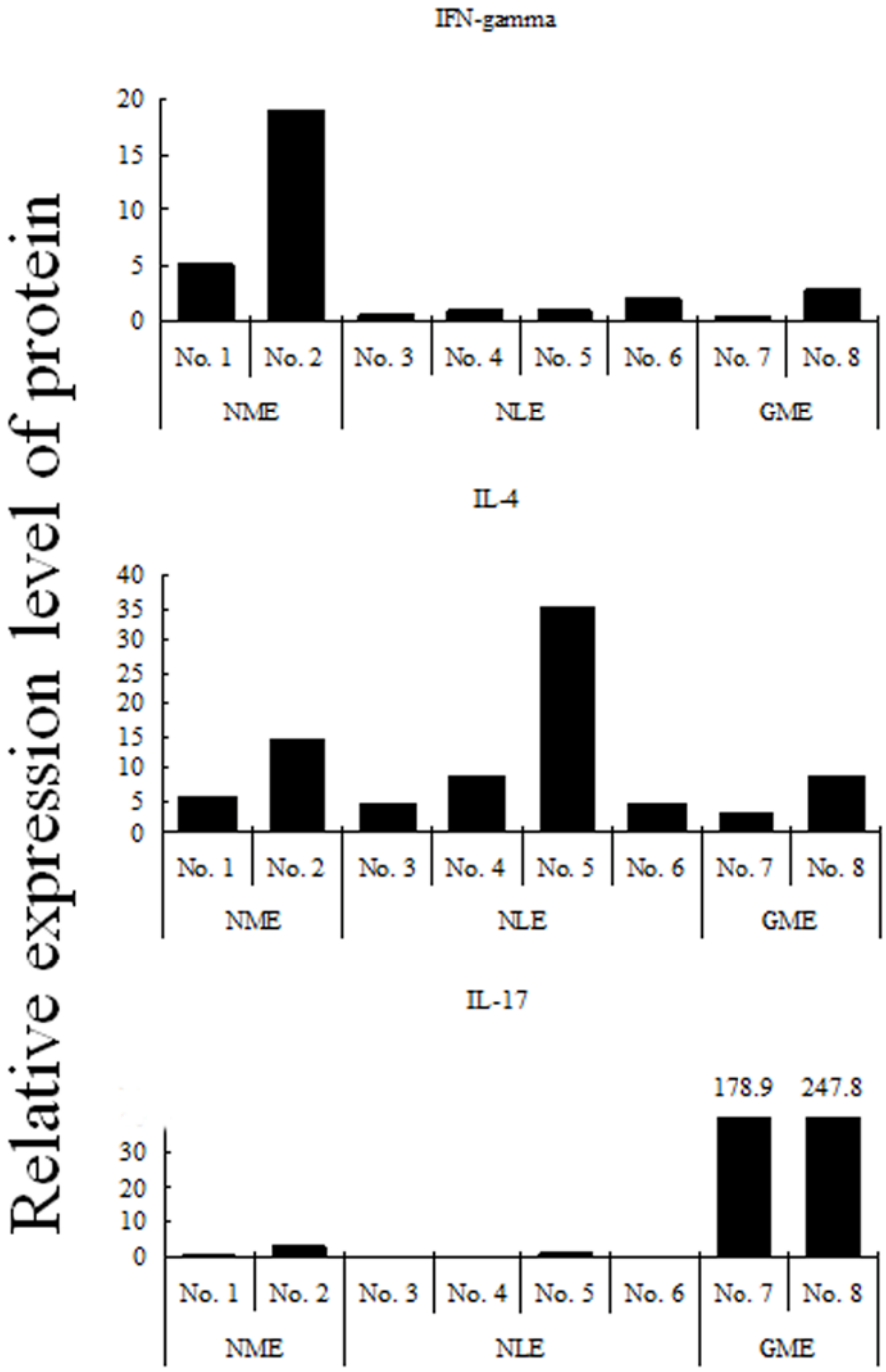

Figure. 3. Protein levels of cytokines by immunoblot analysis.

The relative level of each cytokine protein to that of β-actin was measured and calculated in NME (No. 1 and No. 2), NLE (No. 3, No. 4, No. 5, and No. 6), and GME (No. 7 and No. 8). (upper) IFN-γ. (middle) IL-4. (bottom) IL-17.

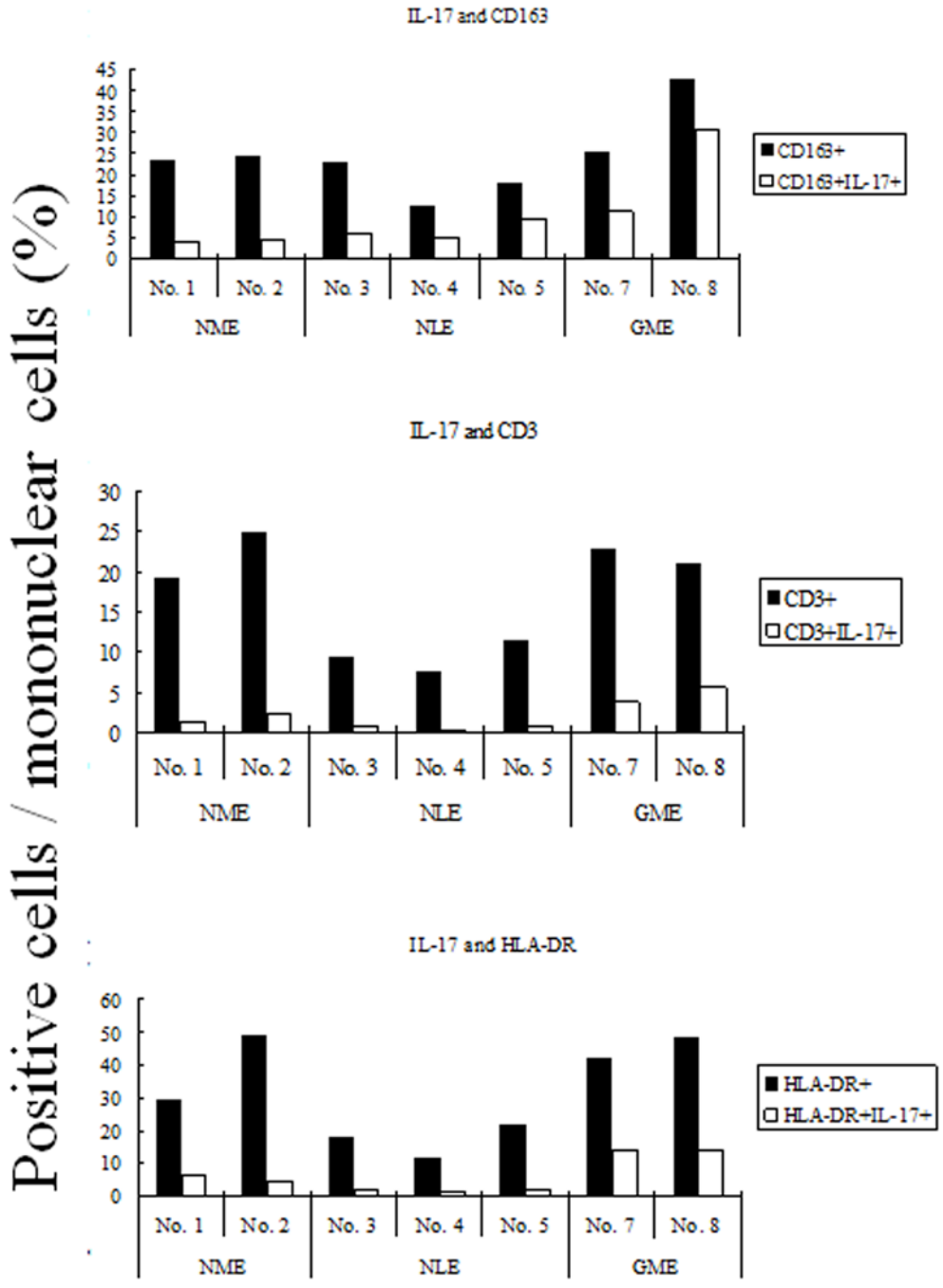

Figure. 4. Percentage of positive cells by double-labeling immunofluorescence. Results are shown as the ratio of single- (black bar) and double- (open bar) positive cells in total mononuclear cells. (upper) IL-17-positive cells and IL-17- and CD163-double positive cells. (middle) IL-17-positive cells and IL-17- and CD3-double positive cells. (bottom) IL-17-positive cells and IL-17- and HLA-DR-double positive cells.

Chapter III

Establishment of a rodent model for canine necrotizing meningoencephalitis (NME), necrotizing leukoencephalitis (NLE) and granulomatous meningoencephalomyelitis (GME).

Summary

The pathogenesis of necrotizing meningoencephalitis (NME), necrotizing leukoencephalitis (NLE) and granulomatous meningoencephalomyelitis (GME) is still uncertain, although they are considered immune-meidated diseases. The purpose of the present study is to generate a rodent model(s) of these diseases. Rats were injected with rat cerebrum or cerebellum homogenates. Rats injected with cerebrum homogenate (Cbr) exhibited vacuolar or malacic changes mainly in the cerebral cortex. CD3-positive T cells and Iba-1-positive CD163-negative microglia infiltrated around the lesions. IgG deposited in the GFAP-positive glia limitans from the early phase, and CD3-positive T cells attached to the GFAP-positive astrocytes. Autoantibody against glial fibrillary acid protein (GFAP) was detected in the sera. These pathological features of Cbr group were consistent with those of canine NME. In contrast, rats injected with cerebellum homogenate (Cbe) exhibited demyelinating lesions with inflammatory reactions in the cerebellum, brain stem and spinal cord. The presence of demyelination and autoantibody against myelin basic protein (MBP) in Cbe group were similar to murine experimental autoimmune encephalitis (EAE), unlike NLE and GME. All the present findings indicate that an autoantibody together with microglia and T cells may play a major role in the pathogenesis of idiopathic canine meningoencephalomyelitis.

Introduction

There are idiopathic necrotizing meningoencephalitis (NE) and granulomatous meningoencephalomyelitis (GME) in dogs. NE is characterized by malacic changes, perivascular cuffs (PC) and the infiltration of inflammatory cells in the neuroparenchyma (NP). NE is divided into two subtypes, necrotizing meningoencephalitis (NME) and necrotizing leucoencephalitis (NLE), according to the distribution of lesions [26]. NME and NLE are likely to be breed-specific [chapter 1, 5, 11, 19, 24, 36, 47, 55, 59, 84, 88, 89, 92]. In contrast, GME is characterized by granulomatous lesions in the cerebral white matter, cerebellum, brain stem and spinal cord [chapter 1], and has been reported in dogs of various breeds.

Although the pathogeneses of these diseases have not been fully understood, it has been considered that they are immune-mediated, because of 1) the identification of autoantibody against glial fibrillary acid protein (GFAP) in NME and NLE, 2) the accumulation of autoreactive T cells and B cells against GFAP in the perivascular cuffs and neuroparenchyma, and 3) no detection of specific pathogens [5, 19, 43, 55, 59, 66, 76, 84, 88, 89, 90, 92, 94]. We evaluated infiltrated inflammatory cells to confirm the differences among these diseases, since it is anyhow difficult to differentiate these diseases histopathologically in some acute or subacute cases [chapter 1]. The proportion of CD20-positive B cells, IgG-positive plasma cells, CD163-positive macrophages and microglia is not different in these diseases, although CD3-positive T cells are significantly major in GME [chapter 1]. IFN-γ and IL-17 were expressed in NME and GME cases, respectively [chapter 2]. However, whether these diseases are distinct diseases each other might be uncertain, since different immune reactions could be produced by the same pathogen [8, 29]. The disruption of the balance of Th1/Th2/Th17 immunity may account for the pathogenesis of these diseases.

Models for NE and GME are needed to confirm their pathogenesis. Murine experimental autoimmune encephalitis (EAE) is a model for human multiple sclerosis (MS) [4, 51]. The autoimmune response against myelin proteins, such as myelin basic protein (MBP), proteolipid protein (PLP) and myelin oligodendrocyte glycoprotein (MOG), was analysed and the changes of the response through the disruption of the balance of the immune response, such as the cytokine expressions and dynamics of inflammatory cells, was examined, using this model [6, 49, 61, 63, 79]. However, autoantibodies against myelin proteins, demyelination and axonal damage associated with EAE were not detected in canine NME, NLE and GME [51, 59, 61, 92].

In the present study, rats injected with allogeneic brain tissues is examined histopathologically and molecular-biologically to develop a suitable model(s) for the canine encephalitis.

Materials and methods

Rat

Eight-week-old male LEW/SsN rats were purchased from SLC (Shizuoka, Japan). The animals were housed in isolator cages under a specific pathogen-free condition. The experimental procedures in the present study were approved by the Experimental Animal Committee of the University of Tokyo.

Immunization using rat brain homogenates

The rat cerebrum and cerebellum were homogenized in PBS, respectively. Ce rebrum (500 μg/μl) and cerebellum (500 μg/μl) homogenates with heat-killed *Mycobacterium tuberculosis* H37RA (Difco Laboratories, Detroit, Michigan, US A) were emulsified in complete Freund's adjuvant (5 mg/ml, Sigma, Satin Louis, MO,

USA). The emulsion was injected s.c. into the lower flanks of rats. The outline of experiment was summarized in Table 1. Body weights and clinical symptoms were daily recorded.

Pathological analysis

The brain and spinal cord were removed from rats euthanized when the loss of body weights and the clinical symptoms were significant. Brain and spinal cord tissues were fixed in 10% neutral-buffered formalin, and subsequently embedded in paraffin, sectioned at 4㎛, and stained with hematoxylin and eosin (HE) or Luxol fast blue-HE (LFB-HE) for microscopic examinations. Some fresh brain tissues were frozen in Tissue-Tek O.C.T. Compound (Sakura Finetek Japan, Tokyo, Japan) and stored at -80°C.

Immunohistochemistry

Immunohistochemistry (IHC) was performed according to our previous study [chapter 1]. Primary antibodies applied were listed in Table 2.

Double-labeling immunofluorescence

Six μm thick-paraffin sections were autoclaved at 121°C for 15 min for antigen retrieval and treated with skimmed milk at 37°C for 40 min to block nonspecific reactions. The first primary antibodies listed in Table 1were employed at 4°C overnight. The sections were then incubated with the second primary antibodies also listed in Table 1, at 37°C for 1 hour. The secondary antibody cocktail was employed at room temperature for 1 hour. The cocktail included fluorescein isothiocyanate–labeled goat anti-rabbit IgG (1:200, Vector Laboratories, Burlingame, CA), fluorescein

isothiocyanate–labeled horse anti-mouse IgG (1:200, Vector Laboratories), Alexa fluor 594-labeled goat anti-mouse IgG (1:200, Invitrogen, Eugene, OR) and Alexa flour 594-labeled donkey anti-rabbit IgG (1:200, Invitrogen). The sections were finally counterstained and mounted with Vectashield HardSet with DAPI (Vector Laboratories), and observed using a Leica DMI3000 B fluorescence microscope.

RNA extraction and cDNA synthesis

Total RNA was prepared by the guanidinium thiocyanate-phenol-chloroform method using the ISOGEN kit (Wako, Osaka, Japan) from the brain and spinal cord tissues, and reverse-transcribed with the PrimeScript® RT-PCR kit (Takara, Otsu, Japan).

Real-time PCR quantification

Real-time PCR on the ABI PRISM (Applied Biosystems, Foster City, CA) was performed in a total volume of 25μl of the SYBR® Green Realtime PCR Master Mix (TOYOBO, Osaka, Japan). Primers used were CCR2, CCR4, CCR6, CXCR3, GAPDH, IFN-γ, IL-4, IL-10, IL-17A, IL-23A, TGF-β and TNF-α (Table 3). PCR reaction was performed on the MicroAmp™ Optical 96-well Reaction Plate (Applied Biosystems) with an initial degeneration step at 54℃ for 30s, at 95℃ for 3m and following 10 cycles at 95℃ for 30s, and an annealing step at 68℃ for 1m, at 72℃ for 30s and following 30 cycles at 95℃ for 30s. At the end of each cycle, the intensity of fluorescence emitted from SYBR Green was measured. After completion of the process, samples were subjected to a dissociation curve analysis (from 5℃ above annealing temperature to 95℃). Samples were then quantified automatically (7900HT version 2.3 Sequence Detection Systems, Applied Biosystems). A single narrow peak was observed by the dissociation curve analysis at the specific melting temperature and

a single band of the predicted size was observed by 2% agarose gel electrophoresis. Result of each case was compared with that of the control group by the ΔΔCt method and relative quantification was performed.

Immunoblot

Normal rat brain and spinal cord tissues were homogenized with the TissueRuptor (QIAGEN, Homebrechtikon, Switzerland) and TissueRuptor disposable probes (QIAGEN) in a buffer containing 10mM Tris-HCl (pH 7.8), 1% NP-40, 0.1% SDS, 150mM NaCl, 1mM EDTA (pH 8.0), proteinase inhibitor cocktail, 2mM Na_3VO_4, 10mM NaF and DW. Lysates were incubated on ice for 30 min and centrifuged at 12000g at 4℃ for 20 min. Proteins in supernatants were separated by SDS-PAGE and were transferred to Immun-Blot® PVDF Membranes (BIO-RAD, Hercules, CA). Membranes were incubated with one of the primary antibodies at 4℃ overnight and then with appropriate secondary antibodies at room temperature for 1 hour. The primary antibodies used were listed in Table 1, and the secondary antibodies were horseradish (HRP)-conjugated goat anti-rat IgG (1:5000, GE Healthcare, Buckinghamshire, UK) and HRP-conjugated donkey anti-rabbit IgG (1:5000, GE Healthcare). Protein bands were visualized with the Amersham ECL Prime Western blotting detection reagent (GE Healthcare, Uppsala, Sweden) using a Molecular Imager® ChemiDox™ XRS+ with Image Lab™ software (BIO-RAD, Tokyo, Japan).

Autoantibodies detection

Sera were collected from rats injected with cerebrum or cerebellum homogenates for the detection of autoantibodies. Ten-μm thick cryostat sections of the rat brain were reacted with the sera at 4°C overnight. A secondary antibody against rat

IgG (Dako, Kyoto, Japan) was employed at room temperature for 40 min. Then, fluorescein streptavidin (1:200, Vector Laboratories) was employed at room temperature for 1 hour. The sections were then incubated with a second primary antibody, mouse monoclonal against human glial filament protein (GFP, prediluted, PROGEN, Heidelberg, Germany) or rabbit polyclonal against human myelin basic protein (MBP, Dako) at 37°C for 1 hour. The secondary antibodies were then employed at room temperature for 1 hour. The secondary antibodies were Alexa fluor 594-labeled goat anti-mouse IgG (1:200, Invitrogen) or Alexa flour 594-labeled donkey anti-rabbit IgG (1:200, Invitrogen). The sections were finally counterstained and mounted with the Vectashield HardSet with DAPI (Vector Laboratories), and observed using a Leica DMI3000 B fluorescence microscope.

Results

Clinical symptoms

Body weights of the cerebrum homogenate-injected (Cbr) group and the cerebellum homogenate-injected (Cbe) group decreased from 8 or 9 days after injection compared to those of control groups (PBS-injected or adjuvant-injected groups) (Fig. 1). Rats injected with cerebrum homogenate showed mild tremor, head tilt and circling without paralysis. However, rats injected with cerebellum homogenate showed posterior paresis or paralysis and tremor. No clinical symptoms appeared in rats of control groups.

Pathological changes

In Cbr group, vacuolar and malacic changes and appearance of gemistocytes were observed particularly in the cerebral cortex (Figs. 2A, 2B). Around the lesions, a

large amount of inflammatory cells infiltrated. Additionally, perivascular cuffs, infiltration of inflammatory cells in the leptomeninges and neuroparenchyma, microgliosis, accumulation of gitter cells and endothelial hyperplasia were distributed mainly in the cerebrum (Figs. 2C, 2D). Inflammatory cell infiltration in the leptomeninges appeared prominently in the frontal lobe of the cerebrum from the early phase (Fig. 2C). These inflammatory lesions were observed also in the hypothalamus, midbrain and basal ganglia (Table 4).

In the Cbe group, lesions were demyelination, microgliosis, perivascular cuffs, inflammatory cell infiltration in the leptomeninges and neuroparenchyma, and endothelial hyperplasia (Figs. 2E, 2F, 2G, 2H). These lesions were restricted to the cerebellum, brain stem and spinal cord (Table 4). Demyelination was marked from the brain stem to the spinal cord (Figs. 2E, 2F).

Immunohistochemical analysis

In the Cbr group, CD3-positive T cells, Iba-1-positive macrophages or microglia and myeloperoxidase-positive neutrophils appeared in the cerebral leptomeninges at first. These cells infiltrated remarkably around the vacuolar or malacic lesions in the cerebral cortex (Figs. 3A, 3B and 3C, Table 4). In the Cbe group, CD3-positive T cells, Iba-1-positive macrophages or microglia and myeloperoxidase-positive neutrophils appeared in the cerebellar leptomeninges and spinal cord in the early phase, and then in the cerebral white matter, midbrain, cerebellum and brain stem (Figs. 3D, 3E, 3F, Table 4).

In both groups, the proportion of CD163-positive macrophages was subtle, and their distribution was restricted in the leptomeninges and perivascular Virchow-Robin spaces, but not in the neuroparenchyma (Figs. 4A, 4B). CD163 (ED2) is a member of

the scavenger receptor cysteine-rich group B (SRCR-B) family and functions as a scavenger receptor [25, 72]. CD163 is expressed in approximately 50% of peritoneal macrophages, a subset of splenic macrophages and macrophages in other tissues but not in monocytes, alveolar macrophages and microglia [25, 72]. CD3-positive T cells, Iba-1-positive CD163-negative microglia and Iba-1-positive CD163-positive macrophages were in close approximity to each other in the leptomeninges and Virchow-Robin space (Figs. 4C, 4D, 4E).

In the Cbr group, CD3-positive T cells and Iba-1-positive macrophages or microglia increased in the perivascular cuffs and the neuroparenchyma from 9 to 15 days post injection (Fig. 5A). In contrast, the proportion of myeloperoxidase-positive neutrophils decreased from 9 to 13 days both in the perivascular cuffs and the neuroparenchyma (Fig. 5A), but neutrophils increased again at 15 days (Fig. 5A). On the contrary, in the Cbe group, the proportion of Iba-1-positive macrophages or microglia mildly increased from 11 to 15 days post injection both in the perivascular cuffs and neuroparenchyma (Fig. 5B). The proportion of CD3-positive T cells once increased at 11 days both in the perivascular cuffs and neuroparenchyma, but decreased at 13 and 15 days (Fig. 5B). The proportion of myeloperoxidase-positive neutrophils decreased from 9 to 13 days, although these cells prominently infiltrated in the neuroparenchyma at 15 days (Fig. 5B).

CD20-positive B cells and IgG-positive plasma cells were not observed in both groups (data not shown).

Expression of cytokines and cytokine receptors

The mRNA levels of cytokines and chemokine receptors in the Cbr and Cbe groups were measured by real-time RT-PCR. The results were shown in Fig. 6. In

the Cbr group (Fig. 6A), the mRNA level of TNF-α was very high in the cerebrum at 9 days post injection. However, the level decreased sharply thereafter. The mRNA levels of IL-23 and IL-17 were low all time in the Cbr and Cbe groups. The mRNA levels of IFN-γ and IL-4 were rather lower. The mRNA levels of IL-10 and TGF-β were mild, although the level of TGF-β in the cerebellum was slightly higher than in the cerebrum. The mRNA level of CCR2 was the highest in the cerebrum, followed by CXCR3 at 9 to 13 days post injection. The mRNA level of CCR4 was high at 9 days, and decreased thereafter. The mRNA level of CCR6 was low at any days.

In the Cbe group (Fig. 6B), the mRNA level of TNF-α was high in the cerebellum. The mRNA level of IL-23 was slightly higher in the cerebrum than in the cerebellum. The mRNA level of IL-17 increased from 11 days and was higher in the cerebellum than in the cerebrum. The mRNA levels of IFN-γ and IL-4 were low, although those were high in the cerebrum at 11 days. The mRNA levels of IL-10 and TGF-β were moderate and increased from 11 days. The mRNA level of CXCR3 increased in the cerebellum with time. The mRNA level of CCR6 was prominent in the cerebellum only at 11 days post injection. The mRNA levels of other chemokine receptors were moderate.

Detection of autoantibodies

Sera from the Cbr group reacted with proteins of 40~50 kDa extracted from the cerebrum, cerebellum and spinal cord, corresponding to GFAP. Bands corresponding to MBP of 20~30 kDa were also detected (Fig. 7A). Sera from the Cbe group reacted with proteins of both 20~30 kDa and 40~50 kDa (Fig. 7A). However, autoantibodies could not be detected in the sera from rats which have shown little symptoms or lesions in both groups and control group (data not shown). Thus, autoantibodies against

GFAP or MBP could be generated in both groups and may be involved in the formation of the lesions.

Sera from rats injected with cerebrum homogenate reacted with GFAP-positive glia limitans of the normal rat cerebrum (Fig. 7B). Also, sera from rats injected with cerebellum homogenate reacted with MBP-positive neuronal fibers in the white matter of the cerebellum and spinal cord (Fig. 7C). Overall, autoantibodies against GFAP and MBP were detected in sera of Cbr and Cbe groups, respectively.

CD3-positive T cells were infiltrated in close proximity to GFAP-positive astrocytes in the lesions, and increased with time in Cbr group (Figs. 8A, 8B). Some parts of the GFAP-positive glia limitans were IgG-positive from the early phase to 15 days (Figs. 8C, 8D). A few IgG-positive plasma cells were observed in close proximity to GFAP-positive astrocytes at 15 days (Fig. 8D). On the contrary, such distributions of CD3-positive T cells and IgG were not observed in Cbe group (data not shown).

Discussion

In the present study, models for canine idiopathic meningoencephalitis, NME, NLE and GME, were generated using rats. As autoantibodies against GFAP were detected in NME and NLE, and the distributions of the lesions were similar between canine encephalitis and EAE, rats were injected with purified GFAP, MBP and MOG proteins in our preliminary studies (data not shown). Rats injected with MBP and MOG showed demyelinating lesions with inflammatory reaction, but not malacic changes, which were consistent with those of EAE, rather than those of NLE and GME. Also, rats injected with GFAP did not show any clinical symptoms and histopathological changes. GFAP is an intracellular protein of astrocytes and is not

exposed to inflammatory cells in a normal condition. The injection with GFAP alone, therefore, could not be enough to provoke diseases. Thus, the rat cerebrum or cerebellum homogenate was used as a crude immunogen in the present study.

In rats with Cbr injection, leptomeningitis in the cerebral cortex was observed at the early phase, followed by vacuolar or malacic change restricted to the cerebral cortex. Other lesions, such as perivascular cuffs and infiltration of inflammatory cells into the neuroparenchyma, were located in the similar regions to those of NME [chapter 1]. The percentages of CD3-positive T cells and Iba-1-positive CD163-negative microglia increased according to time in the Cbr group. These T cells and microglia infiltrated considerably around the vacuolar or malacic lesions of the cerebral cortex. In the lesions of NME and NLE in our previous study, a large amount of CD3-positive T cells and CD163-positive macrophages were observed around the malacic lesions [chapter 1]. In contrast, CD163-positive macrophages were restricted in the subleptomeningeal space or in the Virchow-Robin space and did not infiltrated into the neuroparenchyma in the Cbr group. In these spaces, Iba-1-positive CD163-negative microglia were in close proximity to Iba-1-positive CD163-positive macrophages or CD3-positive T cells. Thus, microglia could be activated by macrophages or T cells [2, 33, 35]. Considering that the lesions in the Cbr group were acute and that those of NME and NLE are chronic, microglia may play a key role in the early phase and macrophages infiltrating into the neuroparenchyma do so in the late or chronic phase.

The mRNA expression of TNF-α and CXCR3 were high in the cerebrum of the Cbr group. In canine NME cases, mRNA of IFN-γ and CXCR3 were highly expressed, indicating the differentiation into Th1 immune response [chapter 2]. On the contrary, the expression of mRNAs of IFN-γ and IL-4 were mild and the differentiation to Th1 and Th2 immune response was subtle in the Cbr group. These results could account

for the acute disease progression in this group. As CXCR3 has been reported to be expressed in the microglia as well as activated T cells such as Th1 cells, the importance of microglia in this group was implied [4, 9, 70]. Also, since these phenomena were more prominent in the cerebrum than in the cerebellum, it could be thought that the disease occurring in the Cbr group affects the cerebrum specifically.

Autoantibodies against GFAP were detected in the sera from Cbr rats from the early phase and IgG was deposited in the GFAP-positive glia limitans. This result was consistent with our observation in dogs that IgG deposited in the glia limitans in acute NME cases [chapter 1]. However, few IgG-positive plasma cells or B cells were observed. Therefore, in the early phase, the association of antibodies against GFAP with the lesions has been indicated. Also, CD3-positive T cells were in close proximity to GFAP-positive astrocytes from the comparatively early phase, and increased with time after injection. As T cells were in close proximity to reactive or damaged astrocytes around the malacic lesions or reactive inflammatory lesions in canine NME and NLE of our previous study, T cells have been considered self-reactive [chapter 1]. Consequently, pathogenesis of the experimental disease by the Cbr injection may be similar to that of canine NME in the acute phase and this disease of rats could be a model for NME. Considering the Cbr model for NME, we can conclude that the vacuolar or malacic lesions appear in the comparatively early phase by T cells and microglia, and that the lesions become severer by IFN-γ or IL-4 secreted from activated T cells.

In the Cbe group, the lesions such as perivascular cuffs, leptomenigitis, microgliosis and inflammatory cell infiltration into the neuroparenchyma were observed in the cerebral white matter, cerebellum, brain stem and spinal cord. The lesions appeared in the leptomeninges of cerebellum and spinal cord in the early phase, and in

the cerebellar neuroparenchyma and cerebral white matter later. Such distribution pattern was consistent with that of NLE and GME [chapter 1, 5, 24, 84]. Iba-1-positive CD163-negative microglia were the most markedly observed, followed by CD3-positive T cells. Same to the Cbr group, Iba-1-positive CD163-positive macrophages were restricted to the subleptomeningeal space or Virchow-Robin space. However, in this group, demyelination lesions with inflammatory response were observed in the brain stem and spinal cord and autoantibodies against myelin proteins were detected in sera. However, in canine NLE and GME, demyelination lesions and autoantibodies against myelin proteins were never detected [chapter 1, 5, 24, 59, 84, 88, 89, 90]. Consequently, the pathogenesis of the Cbe-injected rat was similar to that of EAE, but not to that of GME.

The pathogenesis of NME, NLE and GME remains elusive, though they have been considered to be immune-mediated [5, 19, 43, 55, 59, 66, 76, 84, 88, 89, 90, 92, 94]. Also, it was not certain whether autoantibody against GFAP detected in the CSF or serum would be a cause or a secondary byproduct. Though the present Cbr and Cbe models for the canine diseases are, unfortunately, incomplete, some knowledges were obtained from the models; 1) the importance of autoantibody against GFAP, T cells and microglia in the early phase of the diseases, 2) the appearance of specific vacuolar or malacic lesions in the comparatively early phase, 3) the possibility of NME as an autoimmune disease, and 4) the less possibility of GME as an autoimmune response against cerebellum proteins. To our knowledge, the construction of a model for NME has never been reported until the present. The present results may contribute further development of researches on the canine brain diseases.

Table 1. Summary of the experimental design.

Experimental groups	Number (n) of rats	Injection route	Injection dose	Injection times	Sacrifice days post injection
PBS	3	sc[a]		two times[b]	15
CFA[c]	3	sc	5 μg/μl	two times	15
Cbr[d] + CFA	16	sc	500 μg/μl + 5 μg/μl	two times	9, 11, 13, 15
Cbe[e] + CFA	16	sc	500 μg/μl + 5 μg/μl	two times	9, 11, 13, 15

[a] subcutaneous injection

[b] The interval between injections was 12 d

[c] complete Freund's adjuvant

[d] cerebrum homogenate

[e] cerebellum homogenate

Table 2. Primary antibodies used for immunohistochemistry, immunoblot and double-labeling immunofluorescence

Antibody	Manufacturer	Poly/mono	Dilution
CD3	BD Biosciences, Franklin Lakes, NJ, USA	Mono-mouse anti-rat	1:20~25
CD163	AbD Serotec, Raleigh, NC, USA	Mono-mouse anti-rat	1:50
Iba-1	Wako, Osaka, Japan	Poly-rabbit	1:250~500
Myeloperoxidase	Thermo Scientific, Fremont, CA, USA	Poly-rabbit anti-human	1:100
IgG	Vector Laboratories, Inc., Burlingame, CA, USA	Poly-rabbit anti-rat	1:200
GFAP	Dako, Kyoto, Japan	Poly-rabbit anti-bovine	1:100
GFAP	PROGEN Biotechnik, Heidelberg, Deutch	Mono-mouse anti-human	pre-diluted
MBP	Dako, Kyoto, Japan	Poly-rabbit anti-human	1:100

Table 3. Primers used for real-time RT-PCR

Gene	Accesion No.	Direction	Nucleotide sequence
GAPDH	NG_028301.1	forward	GGCAAGTTCAATGGCACAGT
		reverse	TGGTGAAGACGCCAGTAGACTC
CCR2	NM_021866.1	forward	GGCCACCACACCGTATGA
		reverse	ACATGTTGCCCACAAAACCAA
CCR4	NM_133532.2	forward	ATCGTGCACGCAGTGTTTTC
		reverse	GGGAGCTGAGGACTTTCCAC
CCR6	NM_001013145.1	forward	GGACGATGCGTTGTCATTTTC
		reverse	GTGCCCGGGTTTACTCAGAA
CXCR3	NM_053415.1	forward	TGTACCTTGAGGTCAGTGAACG
		reverse	AGGAGGCTGTAGAGGACTGG
IFN-γ	NM_138880.2	forward	TGCAGGATTTTCATGTCACCAT
		reverse	TGGCATAGATGTGGAAGAAAAGAG
IL-4	NM_201270.1	forward	TGATGGGTCTCAGCCCCCACCTTGC
		reverse	CTTTCAGTGTTGTGAGCGTGGACTC
IL-10	NM_012854.2	forward	GCCAAGCCTTGTCAGAAATGA
		reverse	TTTCTGGGCCATGGTTCTCT
IL-17	NM_001106897.1	forward	TGTCCAAACGCCGAGGCCAA
		reverse	ATTGCGGCTCAGAGTCCAGGGT
IL-23	NM_130410.2	forward	CACCAGTGGGACAAATGGATCT
		reverse	ATACGGGGCACGTCACTTTT
TGF-β	NM_021578.2	forward	AAGTCACCCGCGTGCTAATG
		reverse	CCCGAATGTCTGACGTATTGAA
TNF-α	AF329987.1	forward	TACTGAACTTCGGGGTGATTGGTCC
		reverse	CAGCCTTGTCCCTTGAAGAGAACC

Table 4. Distribution of lesions of rats injected with brain homogenate

	Cbr group		Cbe group	
	Severity	Lesions	Severity	Lesions
Cerebral cortex	++++	Vacuolar changes		
Cerebral white matter	+			
Basal ganglia	++			
Thalamus	++			
Hypothalamus	++++			
Limbic system	++	PC[a], NPI[b]		
Midbrain	+++			
Cerebellum	+		++++	Demyelination, PC, NPI
Brain stem	+		++++	
Spinal cord	+		++++	
Cerebral leptomeninges	++++	Leptomeningitis	++	Leptomeningitis
Cerebellar leptomeninges				Leptomeningitis

[a] Perivascular cuffs, [b] Neuroparenchymal infiltration

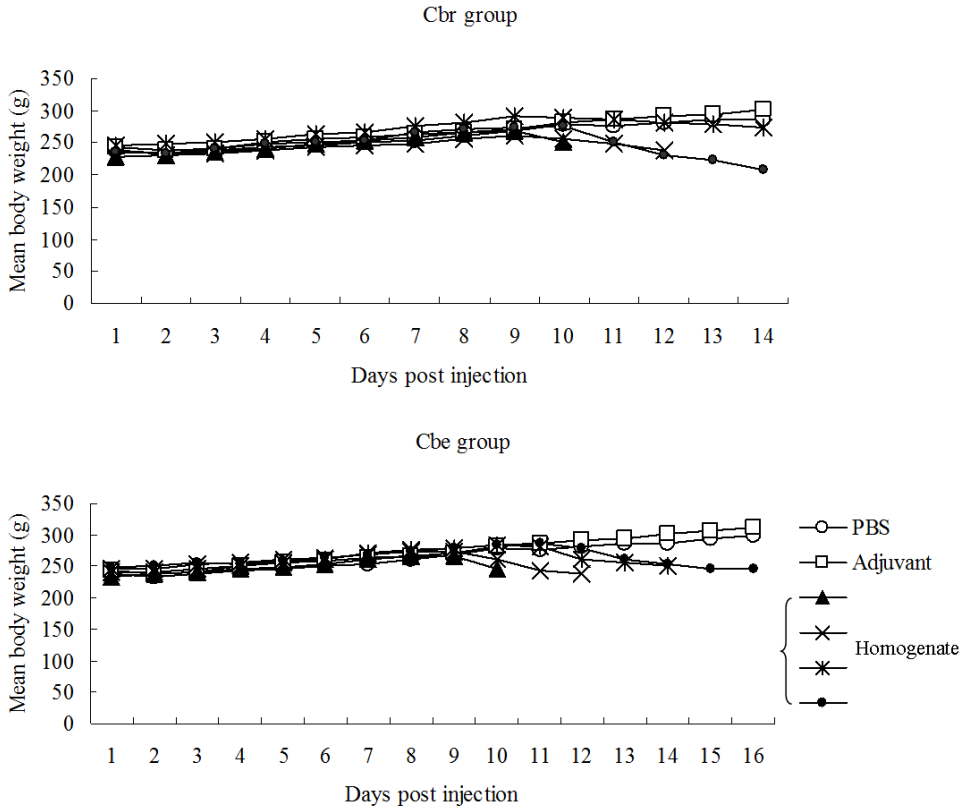

Figure 1. Body weight changes.

The body weight of homogenate-injected rats decreased from 8 days post injection in each group but not in PBS or adjuvant control.

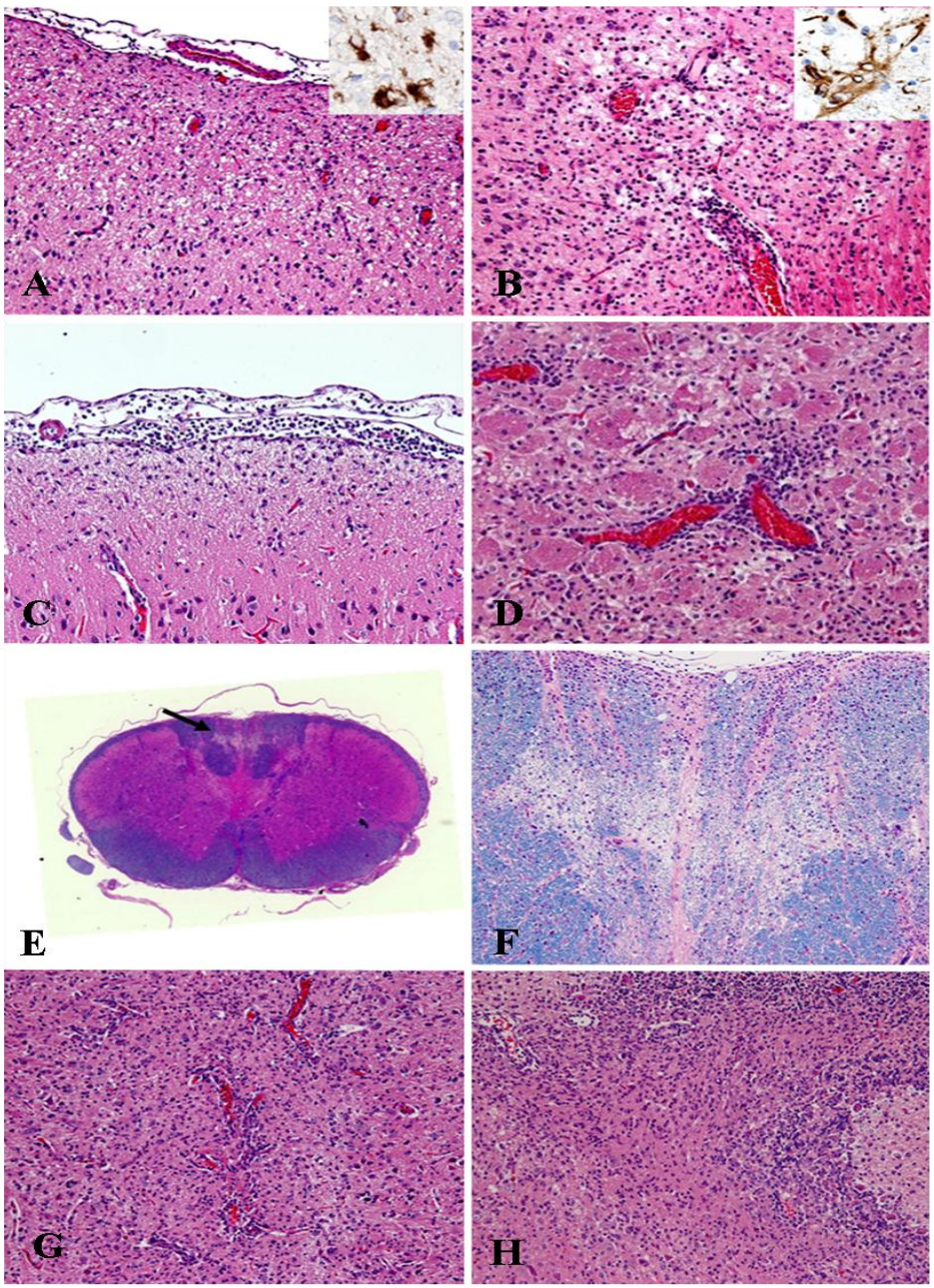

Figure 2. Histological changes of Cbr and Cbe groups.
(A~D) Cbr group. (A) Cerebral cortex; 13pd. Vacuolar changes were prominent. HE. Degenerated astrocytes were observed in the lesions (upper square). IHC, GFAP. (B) Subcortical region; 15pd. Vacuolar or malacic changes were observed. HE. Degenerated or damaged astrocytes were observed in the lesions (upper square). IHC, GFAP. (C) Leptomeninges of the cerebrum; 9pd. Infiltration of inflammatory cells. HE. (D) Basal ganglia; 11pd. Perivascular cuffs and microgliosis were observed. HE. (E~H) Cbe group. (E) Cervical spinal cord; 15pd. Demyelination (arrow) was observed in the dorsal region. LFB-HE. (F) Higher magnification of E. LFB-HE. (G) Cerebellum; 11pd. Perivascular cuffs and endothelial hyperplasia were observed. HE. (H) Cerebellum; 13pd. Infiltration of inflammatory cells and microgliosis were prominent. HE.

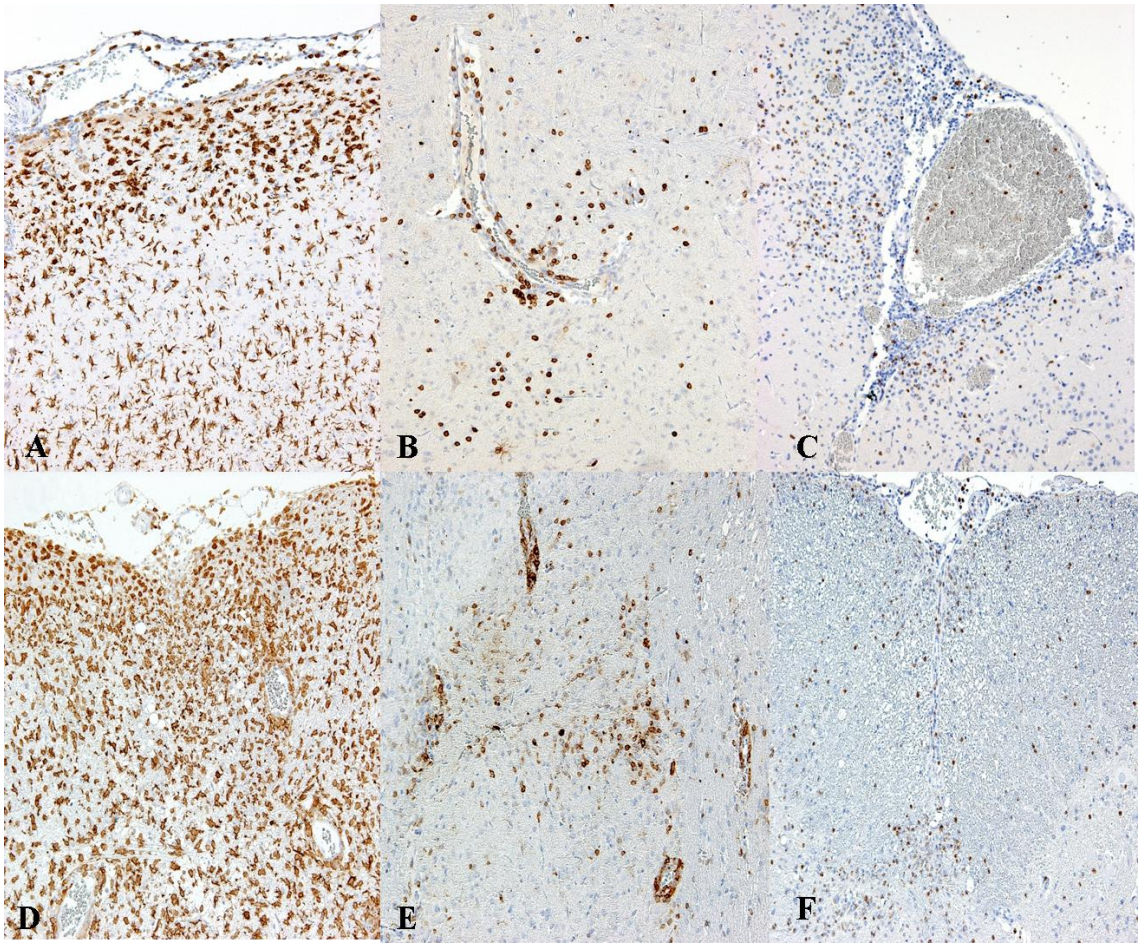

Figure 3. Infiltration of inflammatory cell in rat injected with Cbr or Cbe homogenate.

(A~C) Cbr group. (A) Cerebral cortex; 13pd. Iba-1-positive microglia or macrophages infiltrated in the vacuolar lesions. (B) Cerebral cortex; 15pd. CD3-positive T cells were observed as perivascular cuffs and in the neuroparenchyma. (C) Cerebral cortex; 9pd. Myeloperoxidase-positive neutrophils were observed in the leptomeninges and also infiltrated into the neuroparenchyma. (D~F) Cbe group. (D) Medulla oblongata; 15pd. Iba-1-positive microglia or macrophages infiltrated prominently in demyelinated lesions. (E) Cerebellum; 13pd. CD3-positive T cells were observed as perivascular cuffs and in the neuroparenchyma. (F) Cervical spinal cord; 11pd. Myeloperoxidase-positive neutrophils were sparsely observed in the dorsal region.

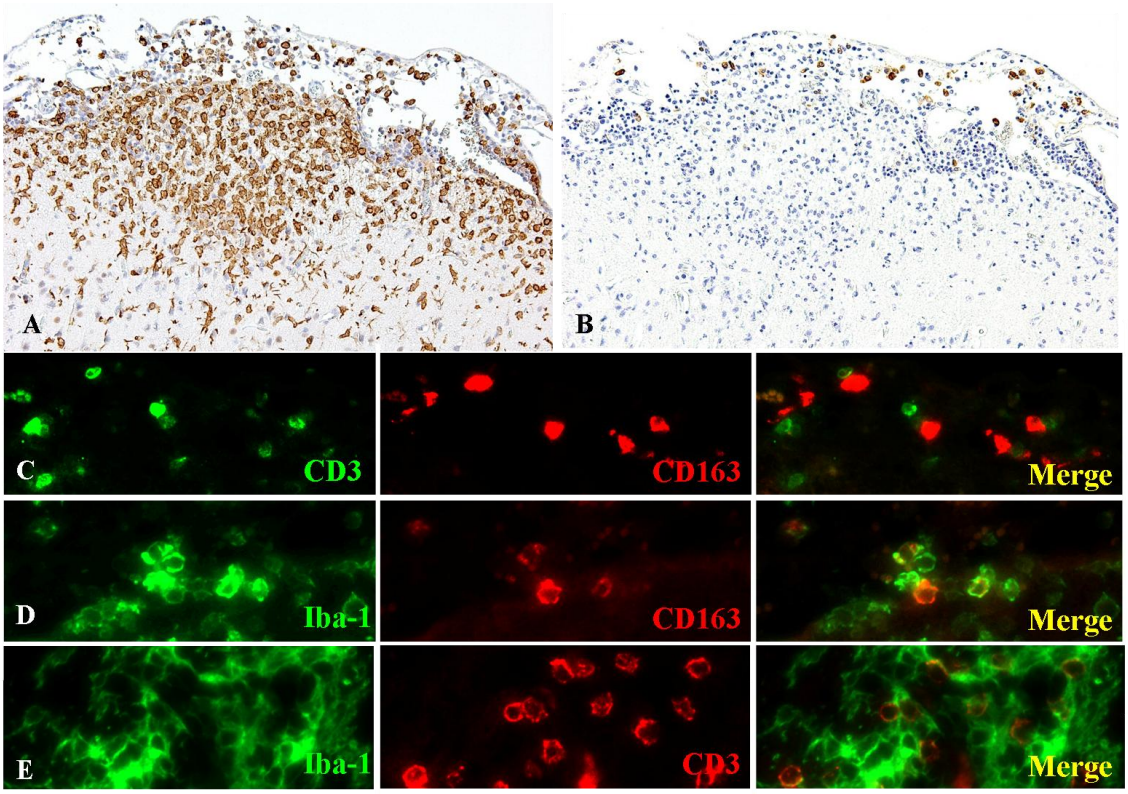

Figure 4. The infiltrations of microglia and macrophages. Cbr group.
(A) Cerebral cortex; 13pd. Iba-1-positive microglia or macrophages diffusely infiltrated in the leptomeninges and the neuroparenchyma. (B) Cerebral cortex; 13pd. CD163-positive macrophages were restricted to the leptomeninges. (C) Leptomeninges of the cerebral cortex; 13pd. CD3-positive T cells were represented as green (left) and CD163-positive macrophages were represented as red (middle), and merged (right). CD3-positive T cells were in close approximity to CD163-positive macrophages. (D) Leptomeninges of the cerebral cortex; 13pd. Iba-1-positive microglia or macrophages were represented as green (left) and CD163-positive macrophages were represented as red (middle), and merged (right). Iba-1-positive CD163-negative microglia were represented as green and Iba-1-positive CD163-positive macrophages were represented as yellow (right). Microglia (green) attached to macrophages (yellow) in the leptomeninges. (E) Cerebral cortex; 15pd. Iba-1-positive microglia or macrophages were represented as green (left) and CD3-positive T cells were represented as red (middle), and merged (right). Iba-1-positive microglia or macrophages were in close to proximity to CD3-positive T cells in the inflammatory lesions.

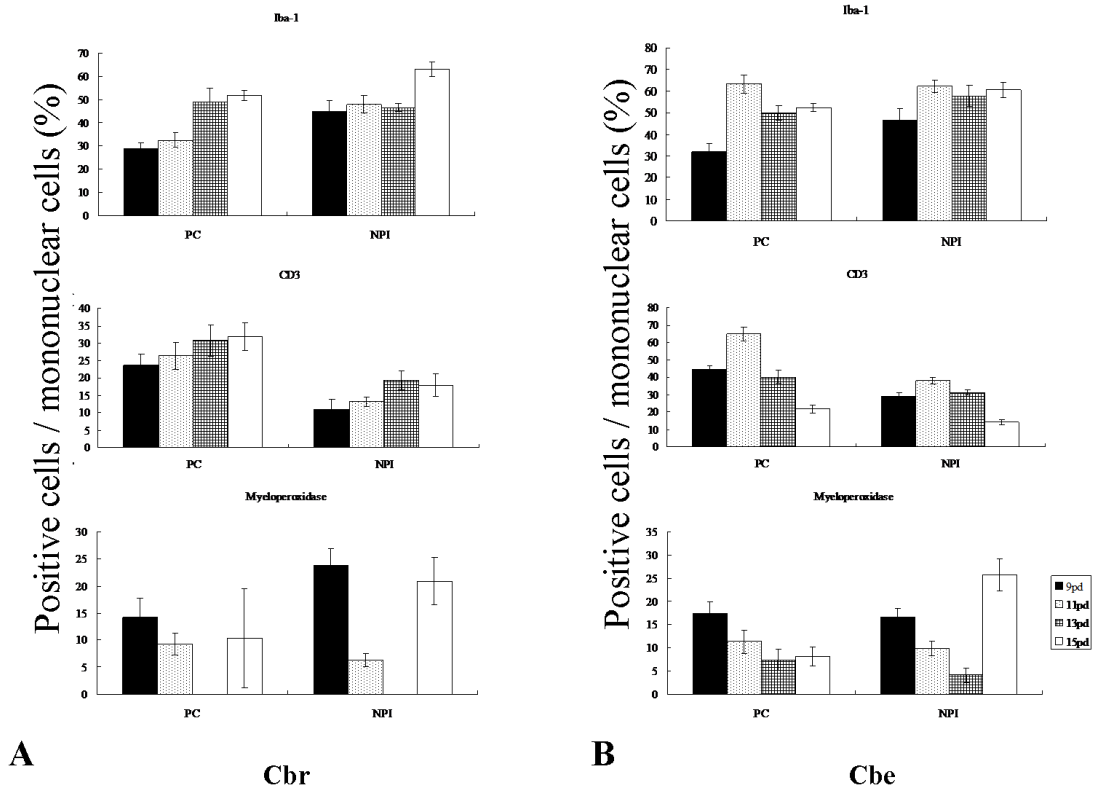

Figure 5. Quantification of inflammatory cells.

The mean percentages of Iba-1-, CD3-, and CD163-positive cells were calculated for perivascular cuffs (PC) and neuroparenchymal infiltration (NPI) in Cbr (A) and Cbe (B) groups with time (9pd~15pd).

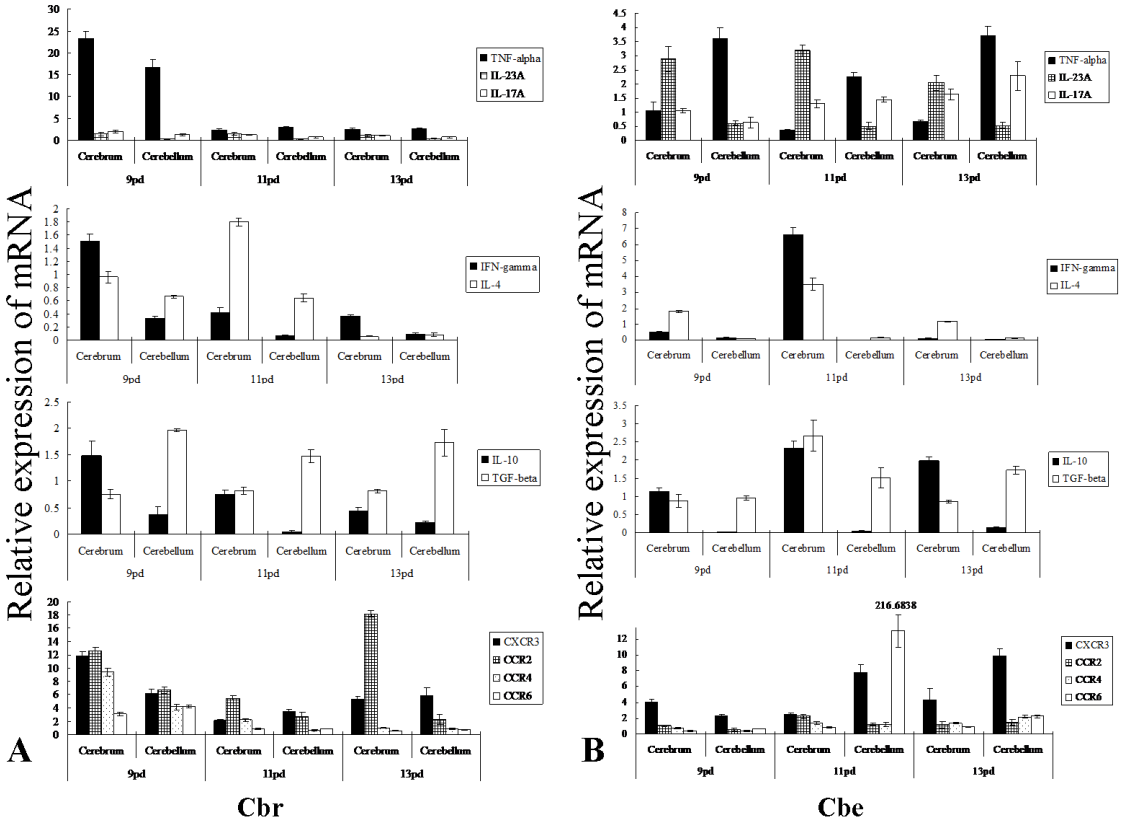

Figure 6. Quantification of mRNA expressions of cytokines and chemokine receptors.

The relative expression levels of mRNA were measured in Cbr (A) and Cbe (B) groups with time (9pd~13pd).

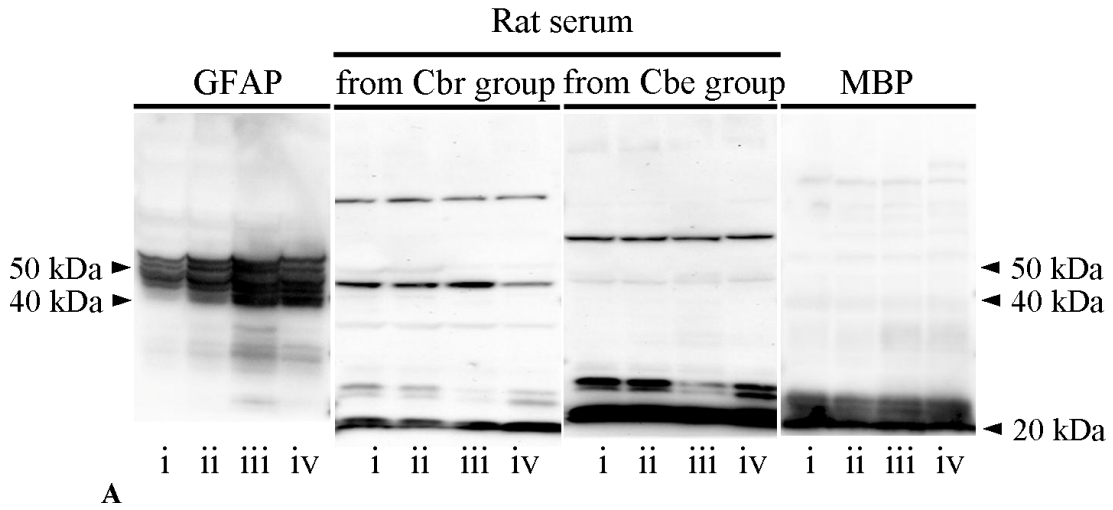

Figure 7. Detection of autoantibodies in sera from Cbr and Cbe groups.

(A) Immunoblot. Proteins of the cerebrum (i and ii), cerebellum (iii) and cervical spinal cord (iv) from normal rats were extracted and electrophoresed. Anti-GFAP, the serum from Cbr group (p15d), the serum from Cbe group (p15d) and anti-MBP were used as the primary antibodies. In Cbr group, strong positive bands were detected between 40 and 50kDa, corresponding to GFAP. Also, there were weak positive bands between 20 and 30kDa, corresponding to MBP. In Cbe group, there were positive bands around 20kDa, corresponding MBP.

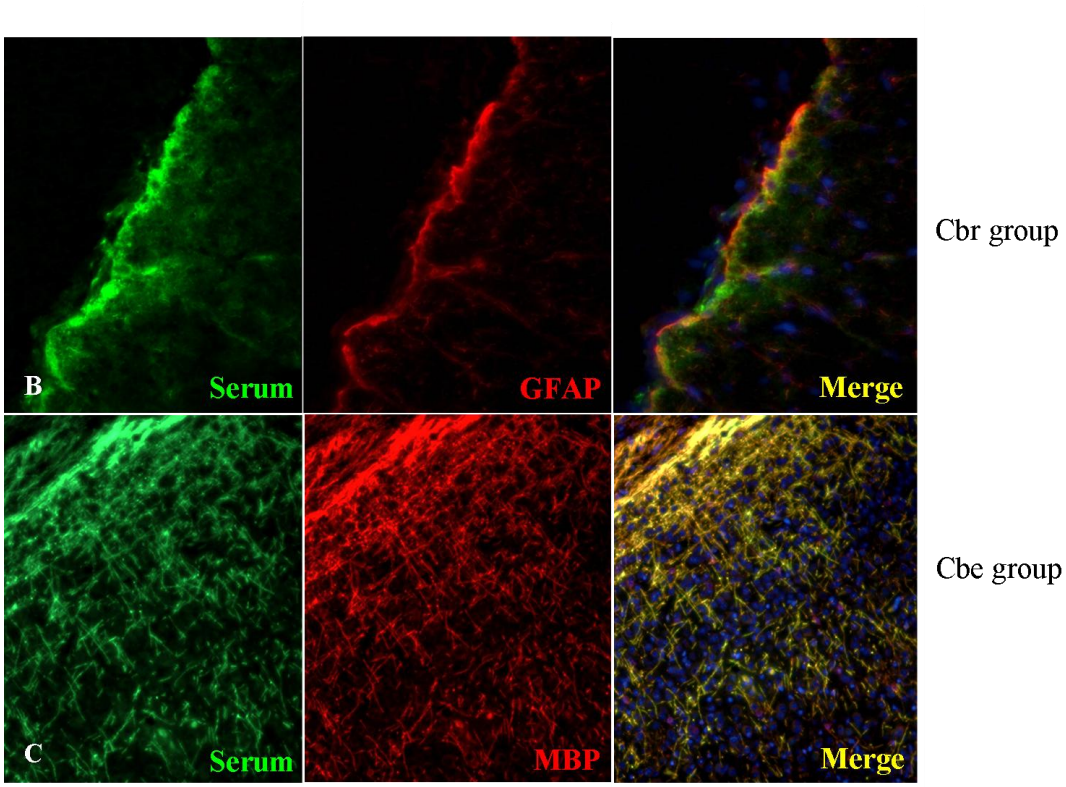

Figure 7. Detection of autoantibodies in sera from Cbr and Cbe groups.

(B~C) Double stain. Sera from Cbr and Cbe groups were applied to the normal rat tissue. (B) Serum (15pd) from Cbr group bound to glia limitans with green signal (left) and GFAP-positive astrocytes and glia limitans were represented with red signal (middle). The co-localization was represented with yellow signal (right). Nuclei were represented with blue signals (DAPI). (C) Serum (15pd) from Cbe group was represented with green signal (left) and MBP-positive myelins were represented with red signal (middle). The colocalization was represented with yellow signal (right). Nuclei were represented with blue signals (DAPI).

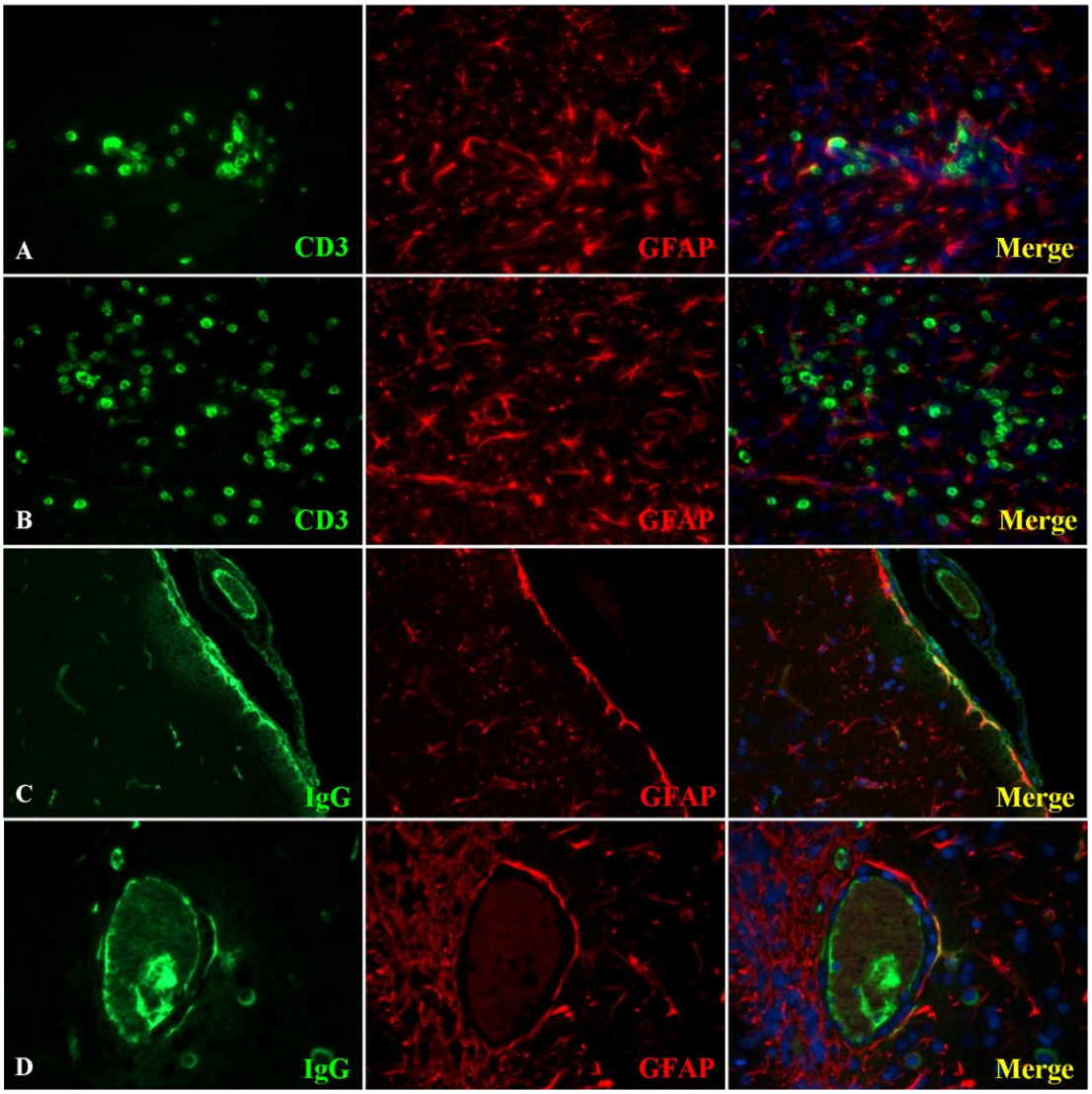

Figure 8. Double-labeling stains. Brain of the Cbr group.
(A) 9 days post injection. CD3-positive T cells were represented as green signals produced by FITC (left), and GFAP-positive astrocytes were represented as red signals produced by Alexa 594 (middle). Merged (right). Nuclei were represented as blue signals produced by DAPI. CD3-positive T cells (green) were in close proximity to GFAP-positive astrocytes (red) in the subcortical region. (B) 15 days. A more large amount of CD3-positive T cells (green) were in close proximity to GFAP-positive astrocytes (red) around the malacic region. (C) 9 days. IgG were represented as green signals produced by FITC (left), and GFAP-positive astrocytes were represented as red signals produced by Alexa 594 (middle). Merged (right). Nuclei were represented as blue signals produced by DAPI. The glia limitans was labeled with both IgG and GFAP (yellow). These double-positive regions appeared from the early phase. (D) 15 days. The processes of astrocytes around the blood vessels were labeled with both IgG and GFAP (yellow) weakly. Also, IgG-positive plasma cells were observed around those regions.

Conclusions

In the Chapter 1, histopathological characteristics such as lesions and the distributions of lesions, and the quantification of inflammatory cells in NE and GME were compared. NME and NLE are two subtypes of NE, according to the distributions of the lesions. In NME, malacic lesions were located in the cerebral cortex and subcortical regions. Other inflammatory lesions were distributed in the thalamus and hippocampus prominently. In NLE, on the contrary, malacic lesions and inflammatory lesions were observed in the cerebral white matter, midbrain, cerebellum and spinal cords. Additionally, NME affected pug, Chihuahua, Maltese and papillon, and NLE affected Yorkshire terriers, consistent with the previous results that these diseases seemed to be breed-specific. In GME, granulomatous lesions, characterized by the accumulation of epithelioid cells, were distributed in the cerebellum, brain stem, spinal cords and cerebral white matter. It was unlikely that GME is breed-specific. It seemed that NE and GME had different characteristic lesions and the etiologies. In the result of the quantification of infiltrating inflammatory cells, the proportion of CD3-positive T cells were significantly different among the three diseases, and was the highest in GME. CD163-positive macrophages diffusely infiltrated around the malacic lesions in NME, and accumulated in the granulomatous lesions in GME. It could be thought that CD163-positive macrophages play a role as scavengers in NME and as effector cells in GME. In NE, IgG was deposited in the GFAP-positive astrocytes, and CD3-positive T cells accumulated around GFAP-positive degenerated astrocytes. These results were not observed in GME. Totally, these canine idiopathic inflammatory disorders of the CNS might be caused by certain genetic factors and multiple immune-mediated mechanisms. In this chapter, the identification of T cell subpopulation, such as helper T1 or T2 cells and cytotoxic T cells, were further analysed

to confirm the distinct immune responses among these diseases. However, due to the limit of antibody availability and the state of tissues, the trial had been failed.

To investigate the difference of characteristic immune responses among these diseases, the expression profiles of cytokines and chemokine receptors were examined in the Chapter 2. IFN-γ, IL-4 and IL-17 were expressed highly in NME, NLE and GME, respectively. As for chemokine receptors, the level of CXCR3 was high in NME and NLE, and that of CCR2 was high in GME. These results could account for or support the results of cytokine expressions. It has been reported that CXCR3-expressing T cells (Th1 cells) produce a large amount of IFN-γ and CCR2-expressing T cells (Th17 cells) produce IL-17. Overall, it is thought that Th1 and Th17 immune responses might be prominent in NME and GME, respectively. As the expression level of IL-17 was the most prominent in GME, IL-17-producing cells in GME were identified using the double-labeling stain. CD163-positive macrophages were the cells most producing IL-17, followed by HLA-DR-positive antigen-presenting cells and CD3-positive T cells. Considering more chronic NE cases, the low expression levels of cytokines or chemokine receptors were observed in the present study. It was reported that astrocytes stimulate the secretion of IFN-γ and IL-17 from T cells and macrophages through the secretion of IL-23. The low expression of IL-17 in NME and NLE may be due to the astrocyte damage. However, the expression level of IFN-γ was higher in NME than GME. Additionally, the proportion of CD163-positive macrophages was not different among these diseases. Totally, the high expression levels of IFN-γ and IL-17 could be specific in NME and GME, and account for the characteristic lesions between these diseases.

In the previous two chapters, the similarities and differences in the histopathological lesions and inflammatory responses among the three diseases were

confirmed. However, the fundamental pathogenesis of the diseases could not be understood yet. As autoantibodies against GFAP were detected in the CSF or serum of NE cases, NE have been considered immune-mediated. Meanwhile, since autoantibodies against GFAP have been detected in the CSF or serum of other brain disorders including GME, it is not certain whether the autoantibody to GFAP is a cause or a secondary product.

Thus, in the Chapter 3, the generation of experimental models for NME, NLE and GME was tried, using rats. In rats with an injection of cerebrum homogenate (Cbr), vacuolar or malacic lesions were observed in the cerebral cortex and the subcortical region early after injection. CD3-positive T cells, and Iba-1-positive and CD163-negative microglia infiltrated prominently around the lesions. The expression levels of TNF-α and CXCR3 were high. This could support an important role of T cells and microglia in the onset of this disease. Also, autoantibody against GFAP was detected in the serum of the rats showing clinical symptoms and lesions. By the double-labeling stain, IgG was detected in the GFAP-positive glia limitans, and CD3-positive T cells were in close proximity to GFAP-positive normal or degenerated astrocytes. These results were consistent with those in NME. Thus, this disease of rats might be an acute model for NME. Through this model, the importance of autoantibodies against GFAP, T cells and microglia in the early phase, and that of the appearance of specific vacuolar or malacic lesions in the comparatively early phase, could have been understood. Also, the possibility of NME as an autoimmune disease was indicated.

On the contrary, in rats with an injection of cerebellum homogenate (Cbe), demyelinated and inflammatory lesions were observed in the cerebral white matter, cerebellum, brain stem and spinal cords. CD3-positive T cells and Iba-1-positive and

CD163-negative microglia were prominent around the lesions. The expression levels of TNF-α and CXCR3 were high, similar to those in the Cbr group. Autoantibodies against MBP were detected in the serum. The distribution of lesions was similar to that in NLE and GME. However, demyelination and autoantibodies against MBP have never been recognized in NLE and GME. Thus, this disease of rats might be experimental autoimmune encephalitis (EAE), rather than a model for NLE or GME. Although the construction of a model for GME was failed, it was indicated that GME may not be caused by the autoimmune response against cerebellum proteins. Considering autoantibodies against GFAP were detected in the CSF from some GME cases, the existence of a common autoantigen between NME and GME might be suspected. There are a few diseases which are caused by different immune responses of Th1 or Th2 to the same pathogen or antigen. Approaches to clarify both a pathogen or antigen and an immune mechanism could be necessary for the construction of a model for GME. This is the first demonstration of the possibility that NME might be caused by an autoimmunity against cerebrum proteins such as GFAP.

To my knowledge, the analysis of cytokine or chemokine receptors among the canine inflammatory brain diseases and the construction of a model for NME have not been reported so far. The present study indicated that these diseases might be caused by distinct immune responses, based on a common autoimmunity and according to the genetic and environmental factors. Further researches on the fundamental development of the autoimmunity against GFAP would be necessary. I hope the present study much contributes to further researches.

Acknowledgement

I wish to express my most sincere gratitude and appreciation to Professor Hiroyuki Nakayama for supervising my doctoral thesis on top of his heavy schedule. Also, I am extremely grateful to Associate Professor Kazuyuki Uchida for his guidance and big generosity to my selfishness and obstinacy, to Dr. Kazuhiko Suzuki and James Chambers for their kind advice and encouragement stimulating me.

This doctoral thesis has standed to benefit from doctors who have been graduated from the Department of Veterinary Pathology, the University of Tokyo. The time discussing with them stimulated me and made me happy. I love all members who accepted me, a foreign student, without resistance as a friend. I could forget tough, sad and hard things when I talked and laughed with them. I never ever forget them in my life, and I wish their success.

References

1. Akagami M, Shibahara T, Yoshiga T, Tanaka N, Yaguchi Y, Onuki T, Kondo T, Yamanaka T, Kubo M. Granulomatous nephritis and meningoencephalomyelitis caused by Halicephalobus gingivalis in a pony gelding. J Vet Med Sci. 69:1187-1190. 2007
2. Aloisi F, Ria F, Adorini L. Regulation of T-cell responses by CNS antigen-presenting cells: different roles for microglia and astrocytes. Immunol Today. 21:141-147. 2000
3. Annunziato F, Cosmi L, Santarlasci V, et al. Phenotypic and functional features of human Th17 cells. J Exp Med. 204:1849-1861. 2007
4. Aranami T, Yamamura T. Th17 Cells and autoimmune encephalomyelitis (EAE/MS). Allergol. Int. 57:115-120. 2008
5. Baiker K, Hofmann S, Fischer A, et al. Leigh-like subacute necrotising encephalopathy in Yorkshire Terriers: neuropathological characterisation, respiratory chain activities and mitochondrial DNA. Acta. Neuropathol. 118:697-709. 2009
6. Banik NL. Pathogenesis of myelin breakdown in demyelinating diseases: role of proteolytic enzymes. Crit Rev Neurobiol. 6:257-271. 1992
7. Becher B, Durell BG, Noelle RJ. Experimental autoimmune encephalitis and inflammation in the absence of interleukin-12. J. Clin. Invest. 110:493-497. 2002
8. Berg AL, Ekman K, Belak S, Berg M. Cellular compositioin and interferon-gamma expression of the local inflammatory response in feline infectious peritonitis (FIP). Vet Microbiol. 111:15-23. 2005
9. Biber K, Dijkstra I, Trebst C, De Groot CJ, Ransohoff RM, Boddeke HW.

Functional expression of CXCR3 in cultured mouse and human astrocytes and microglia. Neuroscience. 112:487-497. 2002

10. Bodil Roth E, Theander E, Londos E, Sandberg-Wollheim M, Larsson A, Sjöberg K, Stenberg P. Pathogenesis of autoimmune diseases: antibodies against transglutaminase, peptidylarginine deiminase and protein-bound citrulline in primary Sjögren's syndrome, multiple sclerosis and Alzheimer's disease. Scand J Immunol. 67:626-631. 2008
11. Bradley GA. Myocardial necrosis in a pug dog with necrotizing meningoencephalitis. Vet. Pathol. 28:91-93. 1991
12. Brand S. Crohn's disease: Th1, Th17 or both? The change of a paradigm: new immunological and genetic insights implicate Th17 cells in the pathogenesis of Crohn's disease. Gut. 58:1152-1167. 2009
13. Breij EC, Brink BP, Veerhuis R, van den Berg C, Vloet R, Yan R, Dijkstra CD, van der Valk P, Bö L. Homogeneity of active demyelinating lesions in established multiple sclerosis. Ann Neurol. 63:16-25. 2008
14. Breuninger LM, Dempsey WL, Uhl J, Murasko DM. Hydrocortisone regulation of interleukin-6 protein production by a purified population of human peripheral blood monocytes. Clin Immunol Immunopathol. 69:205-14. 1993
15. Bromley SK, Mempel TR, Luster AD. Orchestrating the orchestrators: chemokines in control of T cell traffic. Nat Immunol. 9:970-980. 2008
16. Callanan JJ, Mooney CT, Mulcahy G, Fatzer R, Vandevelde M, Ehrensperger F, McElroy M, Toolan D, Raleigh P. A novel nonsuppurative meningoencephalitis in young greyhounds in Ireland. Vet Pathol. 39:56-65. 2002
17. Cañete JD, Martínez SE, Farrés J, et al. Differential Th1/Th2 cytokine patterns in chronic arthritis: interferon gamma is highly expressed in synovium of

rheumatoid arthritis compared with seronegative spondyloarthropathies. Ann. Rheum. Dis. 59:263-268. 2000

18. Cantile C, Chianini F, Arispici M, Fatzer R. Necrotizing meningoencephalitis associated with cortical hippocampal hamartia in a Pekingese dog. Vet Pathol. 38:119-122. 2001
19. Cordy DR, Holliday TA. A necrotizing meningoencephalitis of pug dogs. Vet Pathol. 26:191-194. 1989
20. Cua DJ, Sherlock J, Chen Y, et al. Interleukin-23 rather than interleukin-12 is the critical cytokine for autoimmune inflammation of the brain. Nature. 421:744-748. 2003
21. Daynes RA, Araneo BA. Contrasting effects of glucocorticoids on the capacity of T cells to produce the growth factors interleukin 2 and interleukin 4. Eur J Immunol. 19:2319-25. 1989
22. De Jong EC, Vieira PL, Kalinski P, Kapsenberg ML. Corticosteroids inhibit the production of inflammatory mediators in immature monocyte-derived DC and induce the development of tolerogenic DC3. J Leukoc Biol. 66:201-4. 1999
23. Demierre S, Tipold A, Griot-Wenk ME, et al. Correlation between the clinical course of granulomatous meningoencephalomyelitis in dogs and the extent of mast cell infiltration. Vet. Rec. 148:467-472. 2001
24. Ducoté JM, Johnson KE, Dewey CW, et al. Computed tomography of necrotizing meningoencephalitis in 3 Yorkshire Terriers. Vet. Radiol. Ultrasound. 40:617-621. 1999
25. Fabriek BO, Dijkstra CD, van den Berg TK. The macrophage scavenger receptor CD163. Immunobiology. 210:15-160. 2005
26. Fearnside SM, Kessell AE, Powe JR. Cervical hyperaesthesia in a Maltese

Terrier with necrotising meningoencephalitis. Aust Vet J. 82:550-552. 2004

27. Fisher M. Disseminated granulomatous meningoencephalomyelitis in a dog. Can Vet J. 43:49-51. 2002
28. Fliegner RA, Holloway SA, Slocombe RF. Granulomatous meningoencephalomy-elitis with peripheral nervous system involvement in a dog. Aust Vet J. 84:358-361. 2006
29. Foley JE, Rand C, Leutenegger C. Inflammation and changes in cytokine levels in neurological feline infectious peritonitis. J Feline Med Surg. 5:313-322. 2003
30. Greer KA, Wong AK, Liu H, Famula TR, Pedersen NC, Ruhe A, Wallace M, Neff MW. Necrotizing meningoencephalitis of Pug Dogs associates with dog leukocyte antigen class II and resembles acute variant forms of multiple sclerosis. Tissue Antigens. 76:110-118. 2010
31. Haines JL, Ter-Minassian M, Bazyk A, Gusella JF, Kim DJ, Terwedow H, Pericak-Vance MA, Rimmler JB, Haynes CS, Roses AD, Lee A, Shaner B, Menold M, Seboun E, Fitoussi RP, Gartioux C, Reyes C, Ribierre F, Gyapay G, Weissenbach J, Hauser SL, Goodkin DE, Lincoln R, Usuku K, Oksenberg JR. A complete genomic screen for multiple sclerosis underscores a role for the major histocompatability complex. Nat Genet. 13:469-71. 1996
32. Haines JL, Terwedow HA, Burgess K, Pericak-Vance MA, Rimmler JB, Martin ER, Oksenberg JR, Lincoln R, Zhang DY, Banatao DR, Gatto N, Goodkin DE, Hauser SL. Linkage of the MHC to familial multiple sclerosis suggests genetic heterogeneity. Hum Mol Genet. 7:1229-34. 1998
33. Hanisch UK, Kettenmann H. Microglia: active sensor and versatile effector cells in the normal and pathologic brain. Nat Neurosci. 10:1387-1394. 2007
34. Higgins RJ, Dickinson PJ, Kube SA, et al. Necrotizing meningoencephalitis in

five Chihuahua dogs. Vet. Pathol. 45:336-346. 2008

35. Henning EC, Ruetzler CA, Gaudinski MR, Hu TC, Latour LL, Hallenbeck JM, Warach S. Feridex preloading permits tracking of CNS-resident macrophages after transient middle cerebral artery occlusion. J Cereb Blood Flow Metab. 29:1229-1239. 2009
36. Higgins RJ, Dickinson PJ, Kube SA, Moore PF, Couto SS, Vernau KM, Sturges BK, Lecouteur RA. Necrotizing meningoencephalitis in five Chihuahua dogs. Vet Pathol. 45:336-346. 2008
37. Hirota K, Yoshitomi H, Hashimoto M, et al. Preferential recruitment of CCR6-expressing Th17 cells to inflamed joints via CCL20 in rheumatoid arthritis and its animal model. J. Exp. Med. 204:2803-2812. 2007
38. Höftberger R, Aboul-Enein F, Brueck W, Lucchinetti C, Rodriguez M, Schmidbauer M, Jellinger K, Lassmann H. Expression of major histocompatibility complex class I molecules on the different cell types in multiple sclerosis lesions. Brain Pathol. 14:43-50. 2004
39. Hot A, Miossec P. Effects of interleukin (IL)-17A and IL-17F in human rheumatoid arthritis synoviocytes. Ann. Rheum. Dis. 70:727-732. 2011
40. Hu Y, Ota N, Peng I, et al. IL-17RC is required for IL-17A- and IL-17F-dependent signaling and the pathogenesis of experimental autoimmune encephalomyelitis. J. Immunol. 184:4307-4316. 2010
41. Ito K, Chung KF, Adcock IM. Update on glucocorticoid action and resistance. J Allergy Clin Immunol. 117:522-43. 2006
42. Jurewicz A, Biddison WE, Antel JP. MHC class I-restricted lysis of human oligodendrocytes by myelin basic protein peptide-specific CD8 T lymphocytes. J Immunol. 160:3056-3059. 1998

43. Kipar A, Baumgärtner W, Vogl C, et al. Immunohistochemical characterization of inflammatory cells in brains of dogs with granulomatous meningoencephalitis. Vet. Pathol. 35:43-52. 1998
44. Kitagawa M, Kanayama K, Satoh T, Sakai T. Cerebellar focal granulomatous meningoencephalitis in a dog: clinical findings and MR imaging. J Vet Med A Physiol Pathol Clin Med. 51:277-279. 2004
45. Kitagawa M, Okada M, Watari T, Sato T, Kanayama K, Sakai T. Ocular granulomatous meningoencephalomyelitis in a dog: magnetic resonance images and clinical findings. J Vet Med Sci. 71:233-237. 2009
46. Kobayashi T, Okamoto S, Hisamatsu T, et al. IL23 differentially regulates the Th1/Th17 balance in ulcerative colitis and Crohn's disease. Gut. 57:1682-1689. 2008
47. Kobayashi Y, Ochiai K, Umemura T, et al. Necrotizing meningoencephalitis in pug dogs in Japan. J. Comp. Pathol. 110:129-36. 1994
48. Krumbholz M, Faber H, Steinmeyer F, et al. Interferon-beta increases BAFF levels in multiple sclerosis: implications for B cell autoimmunity. Brain. 131:1455-1463. 2008
49. Kuroda Y, Shimamoto Y. Human tumor necrosis factor-alpha augments experimental allergic encephalomyelitis in rats. J Neuroimmunol. 34:159-164. 1991
50. Kuwamura M, Adachi T, Yamate J, et al. Necrotising encephalitis in the Yorkshire terrier: a case report and literature review. J. Small Anim. Pract. 43:459-463. 2002
51. Lassmann H. Experimental models of multiple sclerosis. Rev Neurol (Paris). 163:651-655. 2007

52. Lassmann H, Brück W, Lucchinetti CF. The immunopathology of multiple sclerosis: an overview. Brain Pathol. 17:210-218. 2007
53. Lassmann H, Ransohoff RM. The CD4-Th1 model for multiple sclerosis: a critical [correction of crucial] re-appraisal. Trends Immunol. 25:132-137. 2004
54. Lassmann H. Models of multiple sclerosis: new insights into pathophysiology and repair. Curr Opin Neurol. 21:242-247. 2008
55. Levine JM, Fosgate GT, Porter B, et al. Epidemiology of necrotizing meningoencephalitis in pug dogs. J. Vet. Intern. Med. 22:961-968. 2008
56. Linden M, Brattsand R. Effects of a corticosteroid, budesonide, on alveolar macrophage and blood monocyte secretion of cytokines: differential sensitivity of GM-CSF, IL-1 beta, and IL-6. Pulm Pharmacol. 7:43-7. 1994
57. Lotti D, Capucchio MT, Gaidolfi E, et al. Necrotizing encephalitis in a Yorkshire Terrier: clinical, imaging, and pathologic findings. Vet. Radiol. Ultrasound. 40:622-626. 1999
58. Ma J, Chen T, Mandelin J, Ceponis A, Miller NE, Hukkanen M, Ma GF, Konttinen YT. Regulation of macrophage activation. Cell Mol Life Sci. 60:2334-2346. 2003
59. Matsuki N, Fujiwara K, Tamahara S, Uchida K, Matsunaga S, Nakayama H, Doi K, Ogawa H, Ono K. Prevalence of autoantibody in cerebrospinal fluids from dogs with various CNS diseases. J Vet Med Sci. 66:295-297. 2004
60. Matyash V, Kettenmann H. Heterogeneity in astrocyte morphology and physiology. Brain Res Rev. 63:2-10. 2010
61. Mayer MC, Meinl E. Glycoproteins as targets of autoantibodies in CNS inflammation: MOG and more. Ther Adv Neurol Disord. 5:147-159. 2012

62. Miljkovic D, Momcilovic M, Stojanovic I, et al. Astrocytes stimulate interleukin-17 and interferon-γ production in vitro. J. Neurosci. Res. 85:3598-3606. 2007

63. Mohindru M, Kang B, Kim BS. Functional maturation of proteolipid protein(139-151)-specific Th1 cells in the central nervous system inexperimental autoimmuneencephalomyelitis. J Neuroimmunol. 155:127-135. 2004

64. Noseworthy JH. Progress in determining the causes and treatment of multiple sclerosis. Nature. 399(6738 Suppl):A40-7. 1999

65. Oda N, Canelos PB, Essayan DM, et al. Interleukin-17F induces pulmonary neutrophilia and amplifies antigen-induced allergic response. Am. J. Respir. Crit. Care Med. 171:12-18. 2005

66. Okamoto M, Kagawa Y, Kamitani W, Hagiwara K, Kirisawa R, Iwai H, Ikuta K, Taniyama H. Borna disease in a dog in Japan. J Comp Pathol. 126:312-317. 2002

67. Paliogianni F, Ahuja SS, Balow JP, Balow JE, Boumpas DT. Novel mechanism for inhibition of human T cells by glucocorticoids. Glucocorticoids inhibit signal transduction through IL-2 receptor. J Immunol. 151:4081-9. 1993

68. Panciera DL, Duncan ID, Messing A, et al. Magnetic resonance imaging in two dogs with central nervous system disease. J. Small Anim. Pract. 28:587–596. 1987

69. Porter BF, Ambrus A, Storts RW. Immunohistochemical evaluation of Mx protein expression in canine encephalitides. Vet Pathol. 43:981-987. 2006

70. Rappert A, Bechmann I, Pivneva T, Mahlo J, Biber K, Nolte C, Kovac AD, Gerard C, Boddeke HW, Nitsch R, Kettenmann H. CXCR3-dependent

microglial recruitment is essential for dendrite loss after brain lesion. J Neurosci. 24:8500-8509. 2004

71. Reboldi A, Coisne C, Baumjohann D, et al. C-C chemokine receptor 6-regulated entry of TH-17 cells into the CNS through the choroid plexus is required for the initiation of EAE. Nat Immunol. 10:514-523. 2009
72. Rezaie P, Male D. Microglia in fetal and adult human brain can be distinguished from other mononuclear phagocytes through their lack of CD163 expression. Neuroembryology. 2:130-133. 2003
73. Risch N. Assessing the role of HLA-linked and unlinked determinants of disease. Am J Hum Genet. 40:1-14. 1987
74. Sato W, Aranami T, Yamamura T. Cutting edge: Human Th17 cells are identified as bearing CCR2+CCR5- phenotype. J Immunol. 178:7525-7529. 2007
75. Sawcer S, Jones HB, Feakes R, Gray J, Smaldon N, Chataway J, Robertson N, Clayton D, Goodfellow PN, Compston A. A genome screen in multiple sclerosis reveals susceptibility loci on chromosome 6p21 and 17q22. Nat Genet. 13:464-8. 1996
76. Schatzberg SJ, Haley NJ, Barr SC, de Lahunta A, Sharp NJ. Polymerase chain reaction screening for DNA viruses in paraffin-embedded brains from dogs with necrotizing meningoencephalitis, necrotizing leukoencephalitis, and granulomatous meningoencephalitis. J Vet Intern Med. 19:553-559. 2005
77. Schulze-Koops H, Kalden JR. The balance of Th1/Th2 cytokines in rheumatoid arthritis. Best Pract. Res. Clin. Rheumatol. 15:677-691. 2001
78. Schwab S, Herden C, Seeliger F, Papaioannou N, Psalla D, Polizopulou Z, Baumgärtner W. Non-suppurative meningoencephalitis of unknown origin in

cats and dogs: an immunohistochemical study. J Comp Pathol. 136:96-110. 2007

79. Selmaj K, Papierz W, Glabinski A, Kohno T. Prevention of chronic relapsing experimental autoimmune encephalomyelitis by soluble tumor necrosis factor receptor I. J Neuroimmunol. 56:135-141. 1995
80. Shahrara S, Huang Q, Mandelin AM. 2nd, Pope RM. Th-17 cells in rheumatoid arthritis. Arthritis Res. Ther. 10:1478-6362. 2008
81. Shibuya M, Matsuki N, Fujiwara K, Imajoh-Ohmi S, Fukuda H, Pham NT, Tamahara S, Ono K. Autoantibodies against glial fibrillary acidic protein (GFAP) in cerebrospinal fluids from Pug dogs with necrotizing meningoencephalitis. J Vet Med Sci. 69:241-245. 2007
82. Song C, Luo L, Lei Z, et al. IL-17-producing alveolar macrophages mediate allergic lung inflammation related to asthma. J. Immunol. 181:6117-6124. 2008
83. Sospedra M, Martin R. Immunology of multiple sclerosis. Annu. Rev. Immunol. 23:683–747. 2005
84. Spitzbarth I, Schenk HC, Tipold A, Beineke A. Immunohistochemical characterization of inflammatory and glial responses in a case of necrotizing leucoencephalitis in a French bulldog. J Comp Pathol. 142:235-241. 2010
85. Stalis IH, Chadwick B, Dayrell-Hart B, et al. Necrotizing meningoencephalitis of Maltese dogs. Vet. Pathol. 32:230-235. 1995
86. Steer JH, Vuong Q, Joyce DA. Suppression of human monocyte tumour necrosis factor-alpha release by glucocorticoid therapy: relationship to systemic monocytopaenia and cortisol suppression. Br J Clin Pharmacol. 43:383-9. 1997
87. Summers BA, Cummings JF, DeLahunta A. Veterinary neuropathology. St.

Louis, Missouri: Mosby; 1995

88. Suzuki M, Uchida K, Morozumi M, et al. A comparative pathological study on canine necrotizing meningoencephalitis and granulomatous meningoencephalomyelitis. J. Vet. Med. Sci. 65:1233-1239. 2003
89. Suzuki M, Uchida K, Morozumi M, et al. A comparative pathological study on granulomatous meningoencephalomyelitis and central malignant histiocytosis in dogs. J. Vet. Med. Sci. 65:1319-1324. 2003
90. Talarico LR, Schatzberg SJ. Idiopathic granulomatous and necrotising inflammatory disorders of the canine central nervous system: a review and future perspectives. J Small Anim Pract. 51:138-149. 2010
91. Tipold A, Fatzer R, Jaggy A, et al. Necrotizing encephalitis in Yorkshire terriers. J. Small Anim. Pract. 34:623–628. 1993
92. Uchida K, Hasegawa T, Ikeda M, et al. Detection of an autoantibody from Pug dogs with necrotizing encephalitis (Pug dog encephalitis). Vet Pathol. 36:301-307. 1999
93. von Praun F, Matiasek K, Grevel V, et al. Magnetic resonance imaging and pathologic findings associated with necrotizing encephalitis in two Yorkshire terriers. Vet. Radiol. Ultrasound. 47:260-264. 2006
94. Weissenböck H, Nowotny N, Caplazi P, Kolodziejek J, Ehrensperger F.J. Borna disease in a dog with lethal meningoencephalitis. Clin Microbiol. 36:2127-2130. 1998
95. Woodroofe MN, Cuzner ML. Cytokine mRNA expression in inflammatory multiple sclerosis lesions: detection by non-radioactive in situ hybridization. Cytokine. 5:583-8. 1993
96. Yoshimura T, Sonoda KH, Ohguro N, et al. Involvement of Th17 cells and the

effect of anti-IL-6 therapy in autoimmune uveitis. Rheumatology (Oxford). 48:347-354. 2009

97. Zhang Y, Barres BA. Astrocyte heterogeneity: an underappreciated topic in neurobiology. Curr Opin Neurobiol. 20:588-594. 2010